

## Time-Resolved Measurements and Master Equation Modelling of the Unimolecular Decomposition of CH<sub>3</sub>OCH<sub>2</sub>

A.J Eskola,<sup>1,2</sup> M.A Blitz,<sup>1,3</sup> M.J. Pilling,<sup>1</sup> P.W Seakins<sup>1</sup> and R.J. Shannon<sup>1</sup>

<sup>1</sup> School of Chemistry, University of Leeds, Leeds, LS2 9JT, UK.

<sup>2</sup> Department of Chemistry, University of Helsinki, P.O. Box 55 (A.I. Virtasen aukio 1), FI-00014 Helsinki, Finland

<sup>3</sup> National Centre for Atmospheric Science, University of Leeds, Leeds, LS2 9JT, UK

## Abstract

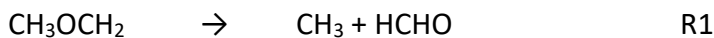
The rate coefficient for the unimolecular decomposition of  $\text{CH}_3\text{OCH}_2$ ,  $k_1$ , has been measured in time-resolved experiments by monitoring the HCHO product.  $\text{CH}_3\text{OCH}_2$  was rapidly and cleanly generated by 248 nm excimer photolysis of oxalyl chloride,  $(\text{ClCO})_2$ , in an excess of  $\text{CH}_3\text{OCH}_3$ , and an excimer pumped dye laser tuned to 353.16 nm was used to probe HCHO via laser induced fluorescence.  $k_1(T,p)$  was measured over the ranges: 573 – 673 K and  $0.1 - 4.3 \times 10^{18}$  molecule  $\text{cm}^{-3}$  with a helium bath gas. In addition, some experiments were carried out with nitrogen as the bath gas.

*Ab initio* calculations on  $\text{CH}_3\text{OCH}_2$  decomposition were carried out and a transition-state for decomposition to  $\text{CH}_3$  and  $\text{H}_2\text{CO}$  was identified. This information was used in a master equation rate calculation, using the MESMER code, where the zero-point-energy corrected barrier to reaction,  $\Delta E_{0,1}$ , and the energy transfer parameters,  $\langle \Delta E_{\text{down}} \rangle \times T^n$ , were the adjusted parameters to best fit the experimental data, with helium as the buffer gas. The data were combined with earlier measurements by Loucks and Laidler (*Can J. Chem.* **1967**, 45, 2767), with dimethyl ether as the third body, reinterpreted using current literature for the rate coefficient for recombination of  $\text{CH}_3\text{OCH}_2$ . This analysis returned  $\Delta E_{0,1} = (112.3 \pm 0.6)$  kJ mol $^{-1}$ , and leads to  $k_1^\infty(T) = 2.9 \times 10^{12} (T/300)^{2.5} \exp(-106.8 \text{ kJ mol}^{-1}/RT)$ . Using this model, limited experiments with nitrogen as the bath gas allowed  $\text{N}_2$  energy transfer parameters to be identified and then further MESMER simulations were carried out, where  $\text{N}_2$  was the buffer gas, to generate  $k_1(T,p)$  over a wide range of conditions: 300 – 1000 K and  $\text{N}_2 = 10^{12} - 10^{25}$  molecule  $\text{cm}^{-3}$ . The resulting  $k_1(T,p)$  has been parameterized using a Troe-expression, so that they can be readily be incorporated into combustion models. In addition,  $k_1(T,p)$  has been parameterized using PLOG for the buffer gases, He,  $\text{CH}_3\text{OCH}_3$  and  $\text{N}_2$ .

## 1. Introduction

The low temperature (500 – 1000 K) combustion of organic compounds involves the initial generation of a radical, R, usually by reaction of the parent molecule with OH. R reacts with O<sub>2</sub> to form a peroxy radical and, following isomerization and further reaction with O<sub>2</sub> chain branching reactions can occur, leading to ignition.[1,2] The mechanism is generally termed *autoignition*. The overall rate of reaction increases with temperature up to where the *negative temperature coefficient* (NTC) range is encountered, when the rate decreases. The NTC results from the shift in the R + O<sub>2</sub> = RO<sub>2</sub> equilibrium and, particularly for ethers, dissociation of the radical, R, competing with its reaction with O<sub>2</sub>. This suppresses branching, because the dissociation products promote autoignition less effectively. Rate coefficients for radical dissociation are essential components of autoignition mechanisms.

Dimethyl ether (DME) is a potential alternative fuel for combustion engines.[3,4] The propagating radical, methoxymethyl, CH<sub>3</sub>OCH<sub>2</sub>, is formed from the OH + DME reaction and dissociates via reaction (R1)



forming the methyl radical which does not undergo low temperature autoignition chemistry. While the kinetics of OH + DME have been widely studied,[5-7] reaction (R1) is much less well characterised.

Loucks and Laidler [8] measured  $k_1$  relative to the rate coefficient for CH<sub>3</sub> + CH<sub>3</sub>, using mercury photosensitisation coupled with end product analysis by gas chromatography.[8] They used a Lindemann Hinshelwood mechanism to analyse their data, reporting the high and low pressure limiting rate coefficient k<sub>1</sub>. Their measurements spanned temperatures of 473 – 573 K and pressures of 4x10<sup>-3</sup> – 0.8 bar; the bath gas was DME. For the high pressure limiting rate coefficient they obtained  $k_1^\infty = 1.6 \times 10^{13} \exp(-106 \text{ kJ mol}^{-1}/RT) \text{ s}^{-1}$ . Sehested et al. [9] used pulse radiolysis coupled with time-resolved uv absorption to study a range of reactions of CH<sub>3</sub>OCH<sub>2</sub> in SF<sub>6</sub> at 18.3 bar and over the temperature range 296 – 666 K. Their results are consistent with the extrapolation of  $k_1^\infty$  from Loucks and Laidler.

Additionally, methoxymethyl decomposition has been investigated using high level electronic structure calculations. Li et al.[10] obtained  $k_1^\infty = 4.45 \times 10^{14} (T/K)^{-0.22} \exp(-13700 \text{ K}/T) \text{ s}^{-1}$  which

lies within a factor of  $\sim 2$  of the results of Loucks and Laidler over the temperature range 400 – 800 K. Gao et al.[11] incorporated multiple structure effects into their calculations to account for torsional and anharmonic effects for the low frequency modes. They obtained  $k_1^\infty = 1.88 \times 10^{12} (T/300 \text{ K})^{1.05} \exp(-11062 \text{ K}/T) \text{ s}^{-1}$ , over the temperature range 450 - 800 K, which is a factor of  $\sim 10$  to  $\sim 3$  greater than the expression of Loucks and Laidler. Gao et al. also used an RRKM analysis to obtain the pressure dependence and the limiting rate coefficients  $k_1^\infty$  and  $k_1^0$ .

Curran et al.[12,13] developed a detailed mechanism for DME pyrolysis and oxidation. They incorporated the Loucks and Laidler[8] high pressure limit value of  $k_1$  but did not include any pressure dependence. They tested the mechanism against the jet stirred reactor studies of Dagaut et al.[14] and found a high negative sensitivity for  $k_1$  at 850 K and 10 atm, but a lower sensitivity at 950 K. Curran et al. subsequently carried out studies in a variable pressure flow reactor (12 – 18 atm, 550 – 850 K) in a nitrogen diluent.[15] Their analysis showed a high negative sensitivity to  $k_1$  at 750 K, but low sensitivity at lower temperatures.

This paper reports the first direct measurements of  $k_1$ , over the temperature range 573 – 673 K in a helium diluent, using pulsed laser photolysis to indirectly, but rapidly, generate  $\text{CH}_3\text{OCH}_2$  with detection of the  $\text{HCHO}$  product with laser induced fluorescence. The results were compared with those from a master equation model, using the code MESMER, based on electronic structure calculations of the reactant and transition state. The best fit was determined by minimising  $\chi^2$  using the barrier height and the temperature dependent energy transfer parameter,  $\langle \Delta E_{\text{down}} \rangle$ , as variable parameters. Parameterized forms are given for  $k_1([M], T)$ .

## 2. Methods

### 2.1 Experimental

Time-resolved studies were conducted in a pulsed photolysis-laser induced fluorescence (LIF) apparatus that has been described in previous publication.[16] Briefly, a stainless steel six-way cross reactor provided the optical axes for the lasers to initiate reaction and for radical detection, where the temperature was set via a central heating block ( $T = 573 - 673\text{ K}$ ). The gases were delivered to the reactor via calibrated mass flow controllers, either directly from a cylinder (He) or via bulbs containing the reagents ( $\text{CH}_3\text{OCH}_3$  and  $(\text{ClCO})_2$ ) diluted with the buffer gas. The pressure of the gases was controlled via a needle valve on the exhaust line and monitored by pressure gauges (MKS) attached to the reactor. Photolysis was initiated by a KrF excimer laser (Lambda Physik, LPX105) that typically gave  $40\text{ mJ/pulse/cm}^2$  output at 248 nm, and generated Cl by photolysis of oxalyl chloride,  $(\text{ClCO})_2$ .[17] The probe laser was a 308 nm excimer (Lambda Physik LPX105) pumped dye laser (Lambda Physik 3002) operating on the dye DMQ to produce light at 353.16 nm.[18] The photolysis and probe light interact only in the centre of the reactor and together define the reaction zone. A thermocouple was located close to the reaction zone. The detection port was perpendicular to the plane defined by the two lasers and the laser induced fluorescence was imaged via a lens and passed through a filter (Perspex) onto the photomultiplier tube (PMT) detector. Formaldehyde, HCHO, has a well-known fluorescence spectrum [19] lying above 350 nm. The fluorescence is short lived, < 50 ns, even at low pressures and is not significantly quenched even at a few hundred Torr of nitrogen. The fluorescence intensity peaks at wavelengths greater than 400 nm, so a Perspex filter (transmits >385 nm) removes laser scatter without significantly decreasing the emission intensity. Further details can be found in Gravestock et al.[18]

A delay generator (SRS, DG 535) was used to delay the probe laser relative to the photolysis laser and the delay time was scanned in order to build up the HCHO time trace, see Figure 1 for an example. The fluorescence detected via the PMT was passed to an oscilloscope (LeCroy, LT262), where it was displayed and integrated before being transferred and stored on a computer. The delay generator and oscilloscope were controlled via LabVIEW and the decay trace was stored for analysis.

Helium (BOC, CP) was used directly from the cylinder. (CICO)<sub>2</sub> (Sigma Aldrich) and DME (Sigma Aldrich) were degassed before dilution in glass bulbs. The total flows were typically ~10 SCCM / Torr, which meant the reaction cell was replenished in ~ 5 seconds (volume of reaction cell ~ 600 cm<sup>3</sup>), independent of the total pressure.

## 2.2 Theory

The analysis relies on master equation simulations with the MESMER software,[20] which requires characterisation of the important species (reactant and transition state) using electronic structure theory. Geometry optimisations were performed for all species at the M06-2X/ 6-31+G\*\* level of theory using the Gaussian 09 software.[21] The energetics for the reaction were refined through single point energy calculations at optimised geometries using the ROHF-UCCSD(T)-F12/aug-cc-pVTZ formalism employed in the Molpro software.[22] As found by Gao et al., the T1 diagnostics for both the well (CH<sub>3</sub>OCH<sub>2</sub>) and TS were found to be below the commonly cited threshold of 0.045, indicating that a single reference method should be appropriate for the current system. To correctly characterise hindered internal rotation of the CH<sub>3</sub> and CH<sub>2</sub> groups, relaxed torsional scans were performed at the M06-2X/ 6-31+G\*\* level of theory for use with the QM hindered rotor methodology used in MESMER.[23] The internal rotor modes were projected from the Hessian and the energy levels calculated based on the numerical potentials.

The calculated molecular parameters were incorporated in the master equation code MESMER and the input file is given in the online supplementary information. A harmonic oscillator – rigid rotor approximation was used for all modes, other than the internal rotors, in determining the ro-vibrational densities of states of each species. The CH<sub>3</sub> and CH<sub>2</sub> torsional motions were projected out of the vibrational Hessian as described by Sharma et al.[24] Energy transfer [25] was treated with an exponential down model and  $\langle \Delta E_{\text{down}} \rangle$ , (the average energy transferred in a downward direction upon collision between CH<sub>3</sub>OCH<sub>2</sub> and either a He, N<sub>2</sub>, or CH<sub>3</sub>OCH<sub>3</sub> bath gas molecule) was used as a fitting parameter in the master equation simulations. Collision rates between CH<sub>3</sub>OCH<sub>2</sub> and the bath were determined using a Lennard-Jones model with the Lennard-Jones parameters  $\epsilon$  and  $\sigma$  determined using the Joback method [26] as implemented in the RMG software suite [27] (see Supplementary Information).

MESMER uses the Levenberg-Marquardt method of fitting, minimising  $\chi^2$  in a comparison of calculated and experimental rate coefficients. The only variable parameters used were the difference in zero point corrected energies between the TS and reactant,  $\Delta E_{0,1}$ , and  $\langle \Delta E_{\text{down}} \rangle$ , which was given a  $T^n$  dependence. The fixed input parameters are given in the SI. MESMER uses matrix techniques and the present analysis is essentially based on the determination in MESMER of the numerically smallest eigenvalue, the single, chemically significant eigenvalue (CSE) for the reaction system. This eigenvalue is well separated from the numerically larger values that relate to internal energy relaxation, so that the use of the CSE to determine  $k_1$  is valid.

### 3. Results

Experiments were carried out using helium as the buffer gas, and the pressures and temperatures were varied over the ranges 7.5 – 280 Torr and 573 - 673 K. The  $\text{CH}_3\text{OCH}_2$  radical was generated via the reaction between chlorine atoms and dimethyl ether:



This reaction is fast, with a rate coefficient  $> 10^{-10} \text{ cm}^3 \text{ molecule s}^{-1}$ ,[28] and exclusively generates  $\text{CH}_3\text{OCH}_2$ . The precursor  $\text{BrCH}_2\text{OCH}_3$  was previously used to generate  $\text{CH}_3\text{OCH}_2$  photolytically,[29] but the yields of  $\text{CH}_3\text{OCH}_2$ , and of other product channels, were not established. As many reactions can generate formaldehyde, reaction R2 better guarantees that the observed HCHO is formed exclusively via R1. In all cases, the conditions were arranged such that the rate of R2 was much greater than that of R1 ( $k_2' \gg k_1'$ ). The exothermicity of reaction R2 (-28 kJ mol<sup>-1</sup>) is much less than the energy required for  $\text{CH}_3\text{OCH}_2$  dissociation, R1, so prompt HCHO formation is not possible.

The formation of HCHO in the system is via reactions R1 and R2, where  $k_2[\text{CH}_3\text{OCH}_3] \gg k_1$ , and HCHO is lost via diffusion to outside the volume, defined by the excimer photolysis beam, cross-section  $2.5 \times 1.0 \text{ cm}^2$ :



The kinetic solution to this scheme is:

$$[\text{HCHO}] = [\text{Cl}]_0 \{(\exp(-k_d t) - \exp(-k_1 t)\} + b \quad \text{E1}$$

where  $[Cl]_0$  is the concentration of Cl generated from the 248 nm photolysis of oxalyl chloride: [30]



At 248 nm, initially a fraction of the photolysis produces ClCO but this decomposes to Cl and CO rapidly at the temperatures of the present experiments.[30] E1 assumes  $CH_3OCH_2$  loss is exclusively via R1 and  $k_d$  is diffusional loss of HCHO. The red line in Figure 1 is the best fit of equation E1 to the data. The  $b$  parameter takes into account background HCHO in the reaction cell.

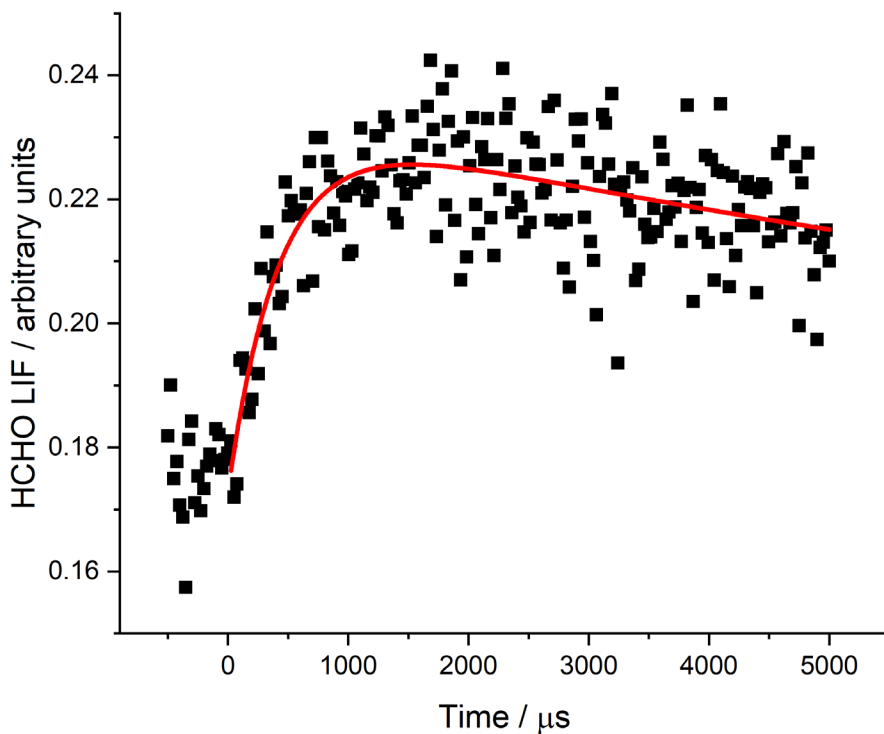


**Figure 1.** An example of the HCHO data at 622 K using helium as the buffer gas. The total pressure was 53.2 Torr,  $(COCl)_2$  and  $CH_3OCH_3$  were equal to  $7.37 \times 10^{14}$  and  $1.39 \times 10^{15}$  molecule  $cm^{-3}$ , respectively. The laser repetition rate was 5Hz while the cell residence time was 5s, so that there is a background of HCHO which can be determined from the signal before zero time (see text).

As expected, the laser induced fluorescence (LIF) signal from HCHO was degraded as the temperature was increased. For this reason  $[\text{CH}_3\text{OCH}_2]$  ( $\sim 10^{13}$  molecule cm $^{-3}$ ) was higher than would normally be used in a LFP/LIF experiments, which implies there was removal of  $\text{CH}_3\text{OCH}_2$  via the self-reaction:



especially at 573 K, where dissociation is slower. The rate coefficient for reaction R4 has been measured at room temperature [9] and above,[31] and it is  $\sim 2 \times 10^{-11}$  cm $^3$  molecule $^{-1}$  s $^{-1}$  at the elevated temperatures of the present experiments, so that  $k_3[\text{CH}_3\text{OCH}_2] \sim 200$  s $^{-1}$ . The impact of the self-reaction, R4, on the observed kinetics is greatest at the lowest temperature, 573 K, where dissociation is slowest and was assessed by analysing traces numerically, including R3 as a second order reaction in  $\text{CH}_3\text{OCH}_2$  with  $[\text{CH}_3\text{OCH}_2] = 1 \times 10^{13}$  molecule cm $^{-3}$ . It was observed that the fitted value returned for  $k_1$  was lowered by  $\sim 200$  s $^{-1}$  compared with the analysis when R4 was omitted. This 200 s $^{-1}$  was subtracted from the observed decay constant to determine  $k_1$  and an additional 200 s $^{-1}$  error was propagated into all the  $k_1$  errors. This results in a large total error at 573 K, but much reduced errors at the higher temperatures, where  $k_1 \sim 10^3 - 2 \times 10^4$  s $^{-1}$ . These total uncertainties are shown in Figs. 2 and 4. The net result is that the 573 K data contribute little to the MESMER analysis.

The detected HCHO is a stable molecule, therefore it was only removed when pumped out of the reaction cell. Typically, the cell is fully replenished every 5 seconds. However, the photolysis light only illuminated a fraction of the cell volume, therefore the laser repetition does not need to be as slow as  $(1/5)$  s $^{-1}$ . In fact, the only requirement is that HCHO from reaction R1 is visible above the background HCHO obtained from previous laser samples, and this requirement was met when the repetition rate was  $\leq 5$  Hz. In Figure 1 the data were collected at 5 Hz, where it can be seen that there is significant residual [HCHO] before time zero.

The experimental results with helium as bath gas are given in Table 1. These results (16 points) were combined with those of Loucks and Laidler (66 points) in a global master equation analysis. Their full dataset was only presented graphically and this was first digitised which potentially introduces some systematic error. Their values of  $k_1$  were determined by end

product analysis, comparing the products of dissociation with those of recombination of  $\text{CH}_3\text{OCH}_2$ . The product ratio is equal to  $k_1/(k_4)^{1/2}$ . The high pressure limiting rate coefficient for  $\text{CH}_3 + \text{CH}_3$  from measurements of Shepp [32] ( $3.7 \times 10^{-11} \text{ cm}^3\text{-molecule}^{-1} \text{ s}^{-1}$ ), was used for  $k_4$  in their analysis. For the present study, these data were recalculated using the rate coefficient for  $\text{CH}_3\text{OCH}_2 + \text{CH}_3\text{OCH}_2$  determined by Maricq et al.[31] The resulting rate coefficients are given in the SI and are each assigned a 20% error.

The master equation analysis, via MESMER, used the zero-point energy corrected barrier with respect to  $\text{CH}_3\text{OCH}_2$ ,  $\Delta E_{0,1}$ , and the temperature dependent energy transfer parameters for helium and DME,  $\langle \Delta E_{\text{down}} \rangle \times T^n$ , to calculate  $k_1$  and compare with the experimental values. MESMER allows fitting to different values of  $\langle \Delta E_{\text{down}} \rangle$  for He and DME in the same global fit. The best fit values of  $k_1(\text{calc})$  are given in Table 1. The best fit parameters, based on minimizing the weighted  $\chi^2$  ( $k_1(\text{calc}) - k_1(\text{expt})$ )<sup>2</sup>, are given in Table 2, where the weight uses the  $k_1$  errors given in Table 1. The value of  $\chi^2$  is 72.5, which implies that the errors in Table 2 are close to  $1\sigma$ . The fits are shown in Figure 2, where lines though the data are from the MESMER fit. The SI provides a comparison of the data from Laidler and Loucks with the results from the best fit model.

The results when  $\text{N}_2$  was the bath gas were incompatible with the present results at higher pressures. This problem arises because of incomplete heat transfer under higher pressure conditions, so that the temperatures recorded on the thermocouples did not accurately record the temperature of the probed reaction zone. The problem was identified by using chemical thermometry, by measuring the rate constant for  $\text{OH} + \text{CH}_4$  under the experimental conditions. This method showed that there were no problems with He as the bath gas, under the conditions studied, because of its higher thermal conductivity. This problem with using nitrogen as the buffer gas has been identified when using a higher pressure system [33] and will be addressed in a future publication.

In our previous publication on  $\text{CH}_3\text{OCH}_2 + \text{O}_2$ ,[34] energy transfer parameters when  $\text{N}_2$  was the buffer gas were determined,  $\langle \Delta E_{\text{down}} \rangle = 523 \pm 53 \text{ cm}^{-1}$  and  $n = 0.01 \pm 0.17$ ,  $(T/298)^n$ . MESMER simulations were made to generate rate coefficients with  $\text{N}_2$  as the buffer gas, using these energy transfer values, coupled with the best fit value for  $\Delta E_{0,1}$  obtained from fitting

the He data. The resulting  $k_1(T,p)$  were parameterized using a Troe expression, and the result is given in Table 2. PLOG parameters are included in the SI.

**Table 1.** Experimental values obtained for  $k_1$  with helium as the buffer gas. The error is equal to  $\pm 20\%$   $k_1$  propagated with an additional error from the contribution from radical - radical reaction with an effective first order rate coefficient of  $200 \text{ s}^{-1}$ . This contribution accounts for the high uncertainties at 573 K. Also tabulated are the calculated  $k_1$  from the MESMER analysis.

$10^{17}[\text{He}] / \text{cm}^{-3}$	T/K	$(k_1/\text{s}^{-1})$ (expt)	error / $\text{s}^{-1}$	$(k_1/\text{s}^{-1})$ (calc)
1.23	573	38	304	124
9.24	573	791	360	392
21.0	573	767	360	584
18.5	573	396	323	551
1.14	622	950	380	560
1.14	622	2750	670	560
8.50	622	1950	520	1943
19.3	622	3350	760	3015
17.0	622	4150	920	2824
43.4	622	5970	1240	4438
1.05	673	1770	500	2011
1.05	673	2520	617	2011
7.87	673	7350	1529	7590
7.87	673	4780	1044	7590
15.8	673	13700	2816	11400
40.1	673	23300	4709	18786

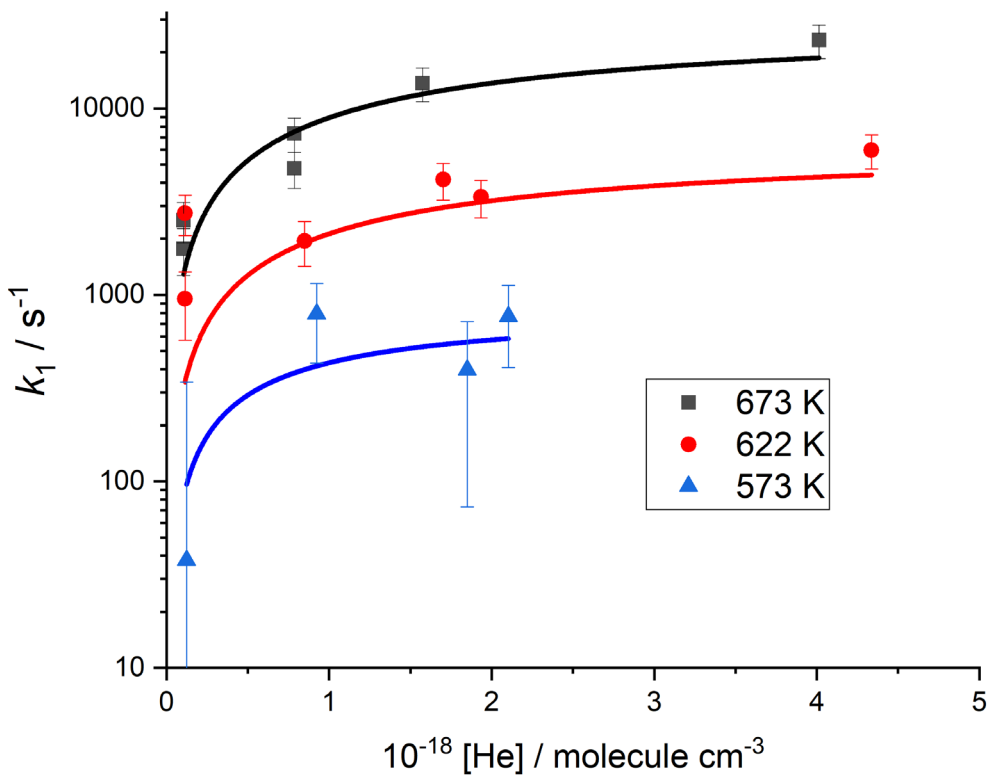


**Figure 2.**  $k_1(T)$  unimolecular decomposition rate coefficient data obtained when helium was the buffer gas.  $k_1$  at a given temperature is behaving in a consistent way as a function of total pressure as evidenced by master equation fitting to the data, the lines through the data.

**Table 2.** MESMER fitted parameters for  $k_1$  together with literature data, and the Troe fitting parameters to the MESMER simulations using N<sub>2</sub> as the buffer gas. The high pressure limit is given in the form:  $k_1(T) = A (T/300)^n \exp(-Ea_1/RT) \text{ s}^{-1}$ . Errors are 1  $\sigma$ .

	This work	Li et al.	Gao <i>et al.</i> <sup>(c)</sup>	Loucks and Laidler <sup>(e)</sup>	Troe parameters (N <sub>2</sub> ) <sup>(f)</sup>
$\Delta E_{0,1} / \text{kJ mol}^{-1}$	$112.5 \pm 0.6^{\text{(a)}}$ $110.8^{\text{(b)}}$		$110.6^{\text{(c)}}$ $111.6^{\text{(d)}}$		
$\langle \Delta E_{\text{down}, \text{He}} \times (T/298)^n / \text{cm}^{-1}$	$195 \pm 320$ $0.77 \pm 2.0$				
$\langle \Delta E_{\text{down,DME}} \times (T/521)^n / \text{cm}^{-1}$	$871 \pm 611$ $-0.87 \pm 1.0$				
$A_1^\infty / \text{s}^{-1}$	$2.89 \times 10^{12}$	$1.27 \times 10^{14}$	$2.08 \times 10^{12}$	$1.6 \times 10^{13}$	$2.19 \times 10^{12}$
$n$	2.51	-0.22	1.002	0	2.77
$Ea_1^\infty / \text{kJ mol}^{-1}$	106.8	113.90	92.27	106.7	106.22
$A_1^0 / \text{s}^{-1}$			$4.1 \times 10^{-8}$	$4.6 \times 10^{-8}$	729
$m$			0.053	0	-8.53
$Ea_1^0 / \text{kJ mol}^{-1}$			75.4	75.7	115.63
$b$					0.469
$x_0$					1.30
$F_{\text{centA}}$					$3.04 \times 10^{-4}^{\text{(f)}}$

<sup>(a)</sup> Results from the MESMER fitting to the experimental results provided here, with He as diluent and from the data of Loucks and Laidler,[8] in DME, rescaled using the data of Maricq et al. for  $k_4$ . <sup>(b)</sup>From Leeds *ab initio* calculations (ROHF-UCCSDT-f12/aug-cc-pVTZ). <sup>(c)</sup> From a G4 calculation. <sup>(d)</sup> From a CCSD(T)/aug-cc-PVTZ//M062X/MG3S calculation. <sup>(e)</sup> The low-pressure limit is for dimethyl ether as the buffer gas. These are the original results given by Loucks and Laidler; the rate coefficients have not been scaled to incorporate the data of Maricq et al. for  $k_4$ . <sup>(f)</sup>  $F_{\text{centB}}$  and  $F_{\text{centC}}$  are equal to zero.

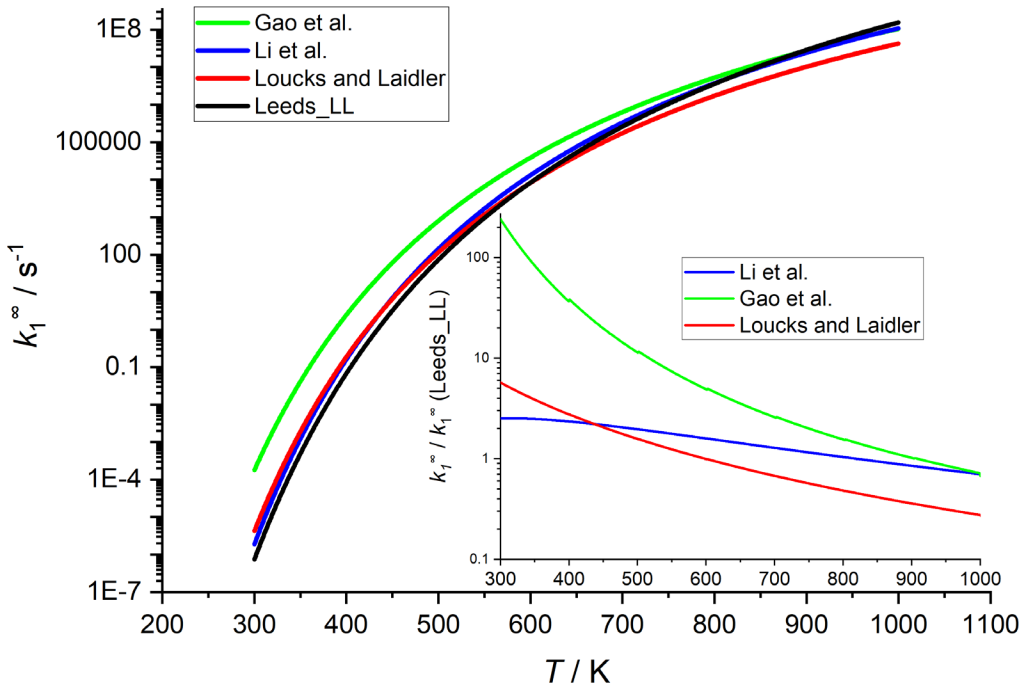


**Figure 3**  $k_1^\infty(T)$  from the literature and this study. The Loucks and Laidler line refers to the parameters from their original study and Leeds\_LL is the result from this study, which includes the Loucks and Laidler data, with the data rescaled using the  $k_4$  values of Maricq et al. The inset shows  $k_1^\infty / k_1^\infty(\text{Leeds\_LL})$ .

#### 4. Discussion

The first study on the thermal decomposition of  $\text{CH}_3\text{OCH}_2$  was the relative rate study by Loucks and Laidler,[8] where the decomposition was carried out between 473 – 573 K with dimethyl ether as the buffer gas. A Lindemann-Hinshelwood expression was used to extrapolate the data to the low and high pressure limiting rate coefficients, which are given in Table 2 and shown in Figure 3. Sehested et al.[9] carried out time-resolved experiments, where  $\text{CH}_3\text{OCH}_2$  was monitored using UV absorption. However, the  $[\text{CH}_3\text{OCH}_2]$  was so high that distinguishing  $k_1$  from self-reaction,  $k_4$ , was not fully resolved and as such their  $k_1$  values just reinforced those of Loucks and Laidler.[8]

The *ab initio* potential energy surface of R1 was calculated by Li et al.[10] and micro-canonical transition-state theory was then used to calculate  $k_1^\infty(T)$ , which is given in Table 2 and shown in Figure 3. Most recently, Gao et al.[11] carried out further calculations on R1, where the calculations were at a higher level and attention was given to the low frequency torsions / anharmonic effects and to tunnelling. Multi-structural canonical variational transition-state calculations were carried out and their  $k_1^\infty(T)$  is given in Table 2 and shown in Figure 3.

Our present results with only the helium data – Table 1 – returned a barrier ( $108.5 \text{ kJ mol}^{-1}$ ) with significant error ( $\pm 8 \text{ kJ mol}^{-1}$ ) when analysed by MESMER. To improve the error in the barrier and the overall parameterisation, the data from Loucks and Laidler were also included in the MESMER calculation, where  $k_1$  was obtained by digitizing their graphical data and converting it to absolute rate coefficients via a more recent determination of  $k_4$ ,[31] the reference reaction in their experiments. The fit parameters from this MESMER analysis are given in Table 2, where it can be seen that the zero temperature barrier to dissociation,  $\Delta E_{0,1}$ , is defined with a small error ( $112.5 \pm 0.6 \text{ kJ mol}^{-1}$ ). This value is in good agreement with our *ab initio* calculation and the calculations by Gao et al.[11], see Table 2. Figure 4 shows a plot of the experimental rate coefficients vs the calculated rate coefficients. The plot shows that the scatter of the Loucks and Laidler data is small, in accordance with the low error in the barrier height when these data are included. The scatter for the Leeds data is greater, but the values are randomly distributed around the line with unit slope in Fig. 4; the direct measurements presented here confirm that no significant systematic error occurs in either the original data of Loucks and Laidler, or in its digitisation and conversion using the Maricq et al. [31] values for  $k_4$ . Figure 4 also shows the three direct measurements by Sehested et al.,[9] which are less compatible with the other data and have not been used in the fits.

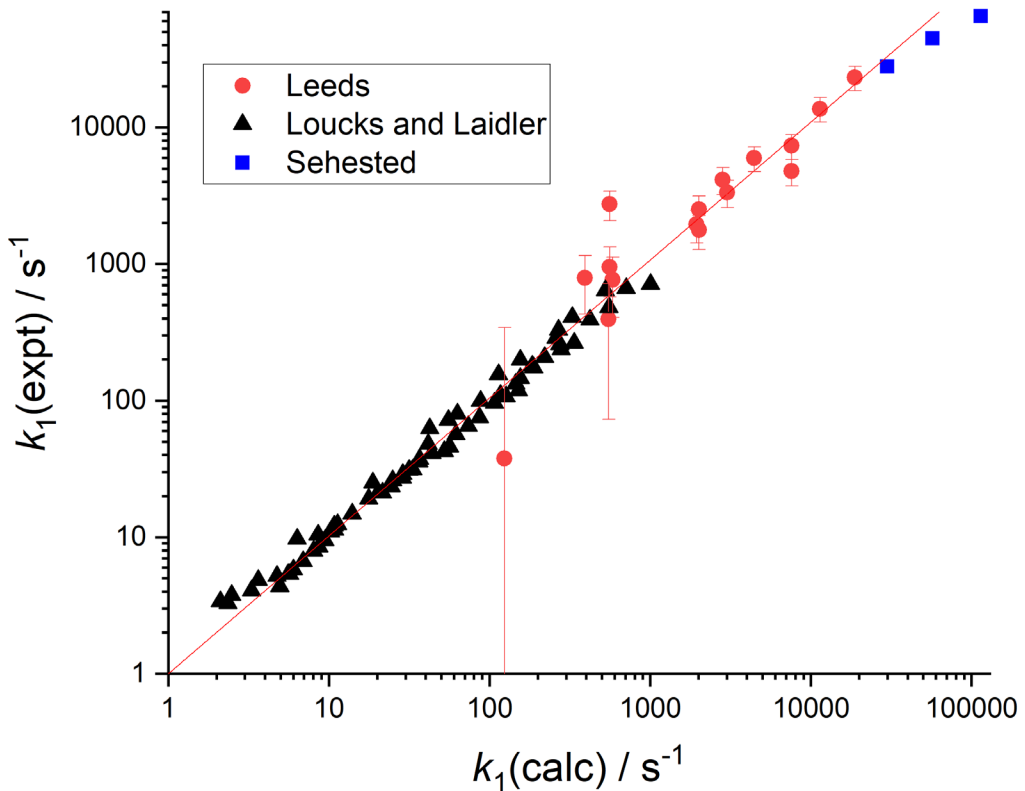


**Figure 4.** Plot of the experimental versus the MESMER best-fit calculated values for  $k_1(T,p)$ . The slope of the line through the data is equal to 1.01, which indicates good agreement. Also included in the plot are the Sehested et al. data.

In our MESMER analysis, energy transfer was adjusted with a temperature dependence,  $\langle \Delta E_{\text{down}} \rangle \times (T/x)^n$ , where  $x$  is either 298 for helium and nitrogen or 521 for dimethyl ether, the centre temperature in the Loucks and Laidler study. While the energy transfer parameters have significant errors (Table 2), there is a strong correlation between the values of  $\langle \Delta E_{\text{down}} \rangle$  and  $n$ . When their covariance is propagated into the calculation of the overall uncertainty for a given bath gas at a specific temperature, the energy transfer is well-defined with an error of  $\sim 10\%$ . The energy transfer values for helium are high but are in agreement with the value in our previous study of the reaction of  $\text{CH}_3\text{OCH}_2$  with  $\text{O}_2$ .[34]

In this MESMER analysis the two lowest frequencies are treated as hindered rotors for both  $\text{CH}_3\text{OCH}_2$  and the transition-state, see Supplementary Information. When the MESMER analysis used a rigid rotor harmonic oscillator model for both  $\text{CH}_3\text{OCH}_2$  and the transition-state, the fit to the data was similar but  $\Delta E_{0,1}$  increased by  $2.5 \text{ kJ mol}^{-1}$ . This effect on  $\Delta E_{0,1}$  of

using hindered rotors in the fit is typical.[35] A fit to the high pressure limit from the MESMER analysis over the temperature range 300 – 1100 K gives  $k_1^\infty(T) = 2.9 \times 10^{12} (T/300)^{2.5} \exp(-106.8 \text{ kJ mol}^{-1}/RT) \text{ s}^{-1}$ .

From Table 2 and Figure 3, our values of  $k_1^\infty$  compare most favourably with the result of Li et al.[10] Our MESMER result is heavily weighted by the Loucks and Laidler data, therefore the difference in Figure 3 between our  $k_1^\infty$  and the original result by Loucks and Laidler is mainly from the more thorough master equation analysis compared with the limited Lindemann-Hinshelwood extrapolation. The biggest difference in Figure 3 is with the results of Gao et al. who employed the most detailed theoretical analysis, using multi-structural variational transition-state theory; they predict a significantly faster  $k_1^\infty$  at low temperatures. It is important to assess the origins of these differences in  $k_1^\infty$ . Our MESMER fitting is based on electronic structure calculations of the vibrational frequencies of the reactant and transition state and incorporates, as discussed above, two hindered internal rotors. Tunnelling was incorporated using an Eckart analysis, with an imaginary frequency of 767 cm<sup>-1</sup>. Since the reaction involves breaking a C-O bond, the reduced mass is high and the effects of tunnelling small (~25% at 500 K). The barrier height was tuned in the fits to the experimental data, and the resulting value agrees well with our calculated barrier height (Table 2). As shown in Figure 4, the best fit to the experimental data is good over a four order of magnitude change in  $k_1$ . As shown in Figure 3, the results of Gao et al. for  $k_1^\infty$  substantially overestimate our best fit values; at 500 K, the difference is over a factor of 10. They used multistructural canonical variational transition state theory, incorporating anharmonicity; they also used two hindered internal rotors. They used multidimensional zero curvature- and small curvature- tunnelling approximations. Although they used a variational model, they noted that the variational effects were negligible. Despite the detailed nature of their model, their results agree poorly with experiment, as represented by our fitted high pressure rate constants. The activation energy in their modified Arrhenius expression is considerably lower than the barrier height, with the major contributions to this lowering deriving from the effects of tunnelling, which increase the rate constant at low  $T$ , and of multistructural effects, which reduce the rate constant at high  $T$ . It is difficult to criticise their analysis on theoretical grounds, but the poor agreement with an extensive experimental dataset necessitates rejection of their final results.

In the intermediate temperature range, where autoignition occurs, the rate coefficients are comparable. At high temperatures, in the NTC range, all the studies have converged, see Figure 3, if the original Loucks and Laidler data are omitted and replaced with the results from the MESMER analysis.

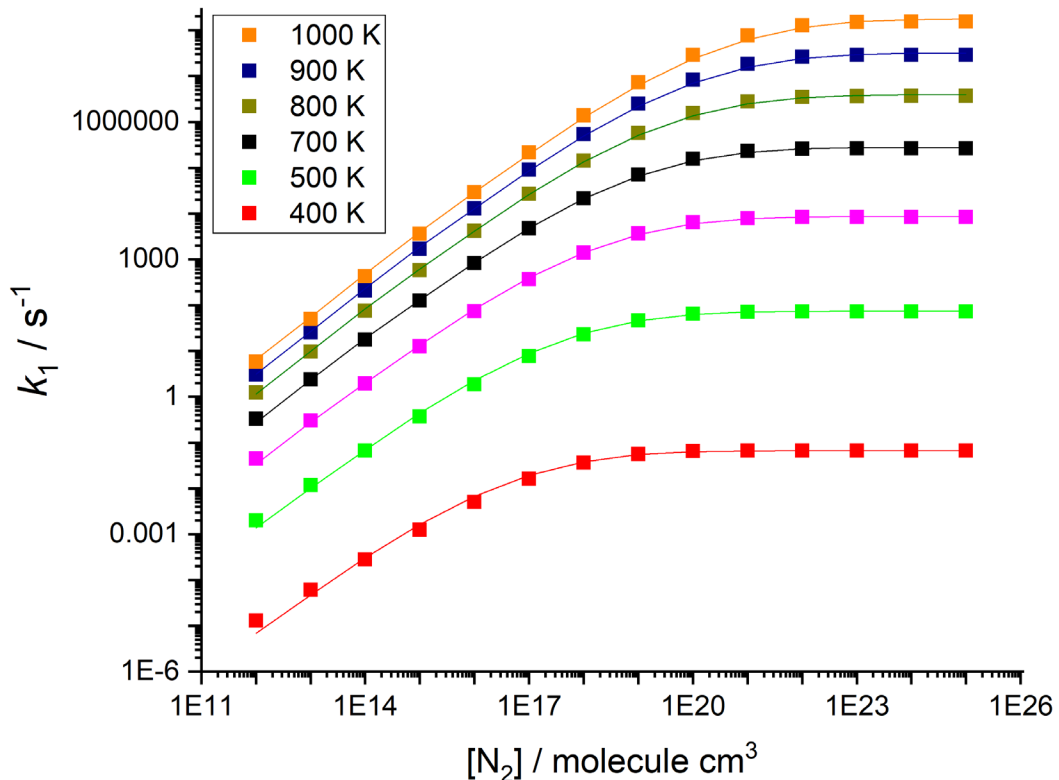


**Figure 5.** Simulated  $k_1(T,p)$  for nitrogen, using the MESMER parameters in Table 2. The line through the  $k_1(T,p)$  data is from a Troe fit, see Table 2 for these parameters.

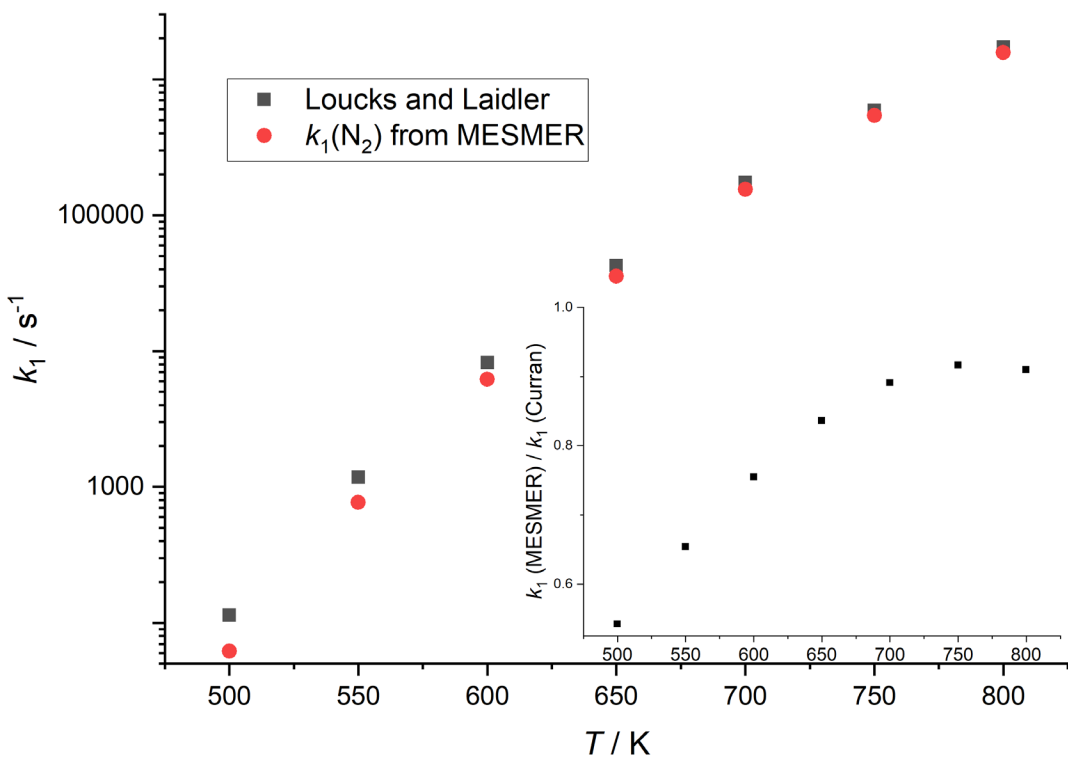


**Figure 6.**  $k_1$  at  $[\text{N}_2] = 10^{20}$  molecule cm<sup>-3</sup> from MESMER versus Loucks and Laidler  $k_1$  used in the dimethyl ether combustion model by Curran et al. [13]. The inset shows  $k_1(\text{MESMER}) / k_1(\text{Curran})$ .

From Table 2, using the energy transfer values for nitrogen, MESMER simulation have been carried out to generate  $k_1$  over a wide ranges of condition. These results have been parameterized using a Troe-type expression [36] and the parameters are given in Table 2. This fitting reproduces the MESMER result with an average error of 3%, and is shown in Figure 5. There are large errors at the lowest pressures and temperatures, but these are under conditions that are not of practical importance. Over the temperature range 400 – 1000 K and for  $[\text{N}_2] = 10^{17} – 10^{21}$  molecule cm<sup>-3</sup>, the maximum difference from unity in the ratio of the Mesmer : Troe rate constants is ~18%. An alternative parameterization is via PLOG analysis and this is presented in the SI for all bath gases considered in the present study, He, CH<sub>3</sub>OCH<sub>3</sub> and N<sub>2</sub>.

The dimethyl ether combustion model developed by Curran et al. [15] was based on experiments carried out in a flow reactor using nitrogen as the buffer gas over the temperature and pressure ranges: 550 – 850 K and 12 – 18 atm. Assuming [N<sub>2</sub>] equal to 10<sup>20</sup>

molecule cm<sup>-3</sup> for the experiments of Curran et al.,[15] the values for  $k_1$  using our MESMER model are compared in Figure 6 with the values from Curran et al., which assumed the original Loucks and Laidler high pressure limiting Arrhenius expression. As can be seen in Figure 6, the values of  $k_1$  are within a factor of three over the whole temperature range, and in good agreement at ~ 800 K. Therefore the dimethyl ether model by Fischer et al. [13] is little affected by our values for  $k_1$  at the reactor pressures used by Curran et al.,[15] but this will not necessarily be true for lower pressures.

While the current experiments on their own do not determine the heat of formation of CH<sub>3</sub>OCH<sub>2</sub>, it can be assigned by considering the study of Gao et al.[11] From Table 2, the two calculations for  $\Delta E_{0,1}$  from Gao et al. are higher and lower than our value, but the associated reaction energy at 0 K from these calculations are 28.5 (G4) and 27.1 kJ mol<sup>-1</sup> (QCISD(T)/aug-cc-pVTZ//MP2/TZVP); so the variation in reaction energy with level of calculation is significantly smaller than the variation in the barrier energies. If these two values for the heat of reaction are combined with the well-known zero K heats of formation of CH<sub>3</sub> (149.9 kJ mol<sup>-1</sup>) and CH<sub>2</sub>O (-105.38 kJ mol<sup>-1</sup>) (uncertainties less than 0.1 kJ mol<sup>-1</sup> [37,38]), then the heat of formation of CH<sub>3</sub>OCH<sub>2</sub> ( $\Delta_f H^0(0\text{ K})$ ) is equal to 16.0 or 17.3 kJ mol<sup>-1</sup>. The uncertainty in this value is down to the reliability of the *ab initio* calculation, which we estimate to be ~ 4 kJ mol<sup>-1</sup>, 1 $\sigma$ . The only previous calculation on the heat of formation CH<sub>3</sub>OCH<sub>2</sub> is by Good and Francisco,[39] who calculated  $\Delta_f H^0(0\text{ K}) = 17.6$  kJ mol<sup>-1</sup> using a lower level of theory. The enthalpy of formation of methoxymethyl at 298 K was discussed by Gao et al., but using outdated enthalpies of formation for methyl and formaldehyde.

## 5. Conclusions

Time-resolved experiments have been carried out to investigate the rate coefficients for unimolecular decomposition of CH<sub>3</sub>OCH<sub>2</sub>,  $k_1$ ; the HCHO product of this reaction was monitored using laser induced fluorescence. The kinetics were determined over a range of temperatures and pressures. These results were analysed using a master equation approach (MESMER) and, to better define the system, the data from Loucks and Laidler [8] were also included in this analysis, after appropriate modification. The reaction barrier was identified with high precision ( $\Delta E_{0,1} = (112.5 \pm 0.6)$  kJ mol<sup>-1</sup>), which is in good agreement with our *ab*

*initio* calculations. MESMER simulations with N<sub>2</sub> as the bath gas, using energy transfer parameters from a previous study, allowed representations of  $k_1(T,p)$  to be determined using both a Troe expression and the PLOG approach, allowing the results to be used in combustion modelling.

## 6. Acknowledgement

A.J.E. acknowledges support from the Academy of Finland, Grant Nos. 130347, 125540, and 288377.

## REFERENCES

- [1] M.J. Pilling, S.H. Robertson, P.W. Seakins, J. Chem. Soc., Faraday Trans. **91** (1995) 4179.
- [2] J. Zador, C.A. Taatjes, R.X. Fernandes, Prog. Energy Combust. Sci. **37** (2011) 371.
- [3] S.H. Park, C.S. Lee, Prog. Energy Combust. Sci. **39** (2013) 147.
- [4] G. Thomas, B. Feng, A. Veeraragavan, M.J. Cleary, N. Drinnan, Fuel Process. Technol. **119** (2014) 286.
- [5] C. Bansch, J. Kiecherer, M. Szori, M. Olzmann, J. Phys. Chem. A **117** (2013) 8343.
- [6] S.A. Carr, T.J. Still, M.A. Blitz, A.J. Eskola, M.J. Pilling, P.W. Seakins, et al, J. Phys. Chem. A **117** (2013) 11142.
- [7] M. Kawade, A. Sharma, D. Srinivas, A. Saha, H.P. Upadhyaya, A. Kumar, et al, Chem. Phys. Lett. **706** (2018) 558.
- [8] L.F. Loucks, K.J. Laidler, Can. J. Chem. **45** (1967) 2767.
- [9] J. Sehested, K. Sehested, J. Platz, H. Egsgaard, O.J. Nielsen, Int. J. Chem. Kinet. **29** (1997) 627.
- [10] Q.S. Li, Y. Zhang, S. Zhang, J. Phys. Chem. A **108** (2004) 2014.
- [11] J. Gao, Y. Guan, J. Lou, H. Ma, J. Song, Combust. Flame **197** (2018) 243.
- [12] H.J. Curran, W.J. Pitz, C.K. Westbrook, P. Dagaut, J.C. Boettner, M. Cathonnet, Int. J. Chem. Kinet. **30** (1998) 229.
- [13] S.L. Fischer, F.L. Dryer, H.J. Curran, Int. J. Chem. Kinet. **32** (2000) 713.
- [14] P. Dagaut, J. Luche, M. Cathonnet, Combust. Sci. Technol. **165** (2001) 61.
- [15] H.J. Curran, S.L. Fischer, F.L. Dryer, Int. J. Chem. Kinet. **32** (2000) 741.
- [16] D.G. Potter, M.A. Blitz, P.W. Seakins, Chem. Phys. Lett. **730** (2019) 213.
- [17] A.V. Baklanov, L.N. Krasnoperov, J. Phys. Chem. A **105** (2001) 97.
- [18] T.J. Gravestock, M.A. Blitz, W.J. Bloss, D.E. Heard, ChemPhysChem **11** (2010) 3928.
- [19] C. Brackmann, J. Nygren, X. Bai, Z.S. Li, H. Bladh, B. Axelsson, et al, Spectroc. Acta Pt. A-Molec. Biomolec. Spectr. **59** (2003) 3347.
- [20] D.R. Glowacki, C.H. Liang, C. Morley, M.J. Pilling, S.H. Robertson, J. Phys. Chem. A **116** (2012) 9545.
- [21] M.J. Frisch, G.W. Trucks, H.B. Schlegel, G.E. Scuseria, M.A. Robb, J.R. Cheeseman, et al, Gaussian 09. Gaussian, Inc., Wallingford CT, 2016, 2009.
- [22] H.J. Werner, P.J. Knowles, G. Knizia, F.R. Manby, M. Schutz, Wiley Interdiscip. Rev.-Comput. Mol. Sci. **2** (2012) 242.
- [23] S.H. Robertson, D.R. Glowacki, C.-H. Liang, C. Morley, R.J. Shannon, M.A. Blitz, et al. MESMER (Master Equation Solver for Multi-Energy Well Reactions), 2008-2013; an Object Oriented C++ Program Implementing Master Equation Methods for Gas Phase Reactions with Arbitrary Multiple Wells. [cited 2019] Available from: <http://sourceforge.net/projects/mesmer>.
- [24] S. Sharma, S. Raman, W.H. Green, J. Phys. Chem. A **114** (2010) 5689.
- [25] S.H. Robertson, Part 2: Collisional Energy Transfer and The Master Equation, ELSEVIER, 2019.
- [26] K.G. Joback, R.C. Reid, Chem. Eng. Commun. **57** (1987) 233.
- [27] C.W. Gao, J.W. Allen, W.H. Green, R.H. West, Comput. Phys. Commun. **203** (2016) 212.
- [28] J.V. Michael, D.F. Nava, W.A. Payne, L.J. Stief, J. Chem. Phys. **70** (1979) 3652.
- [29] A.J. Eskola, S.A. Carr, M.A. Blitz, M.J. Pilling, P.W. Seakins, Chem. Phys. Lett. **487** (2010) 45.
- [30] B. Ghosh, D.K. Papanastasiou, J.B. Burkholder, J. Chem. Phys. **137** (2012) 12.
- [31] M.M. Maricq, J.J. Szente, J.D. Hybl, J. Phys. Chem. A **101** (1997) 5155.
- [32] A. Shepp, J. Chem. Phys. **24** (1956) 939.
- [33] T.H. Speak, M.A. Blitz, D. Stone, P.W. Seakins, Atmos. Meas. Tech. **13** (2020) 839.
- [34] A.J. Eskola, S.A. Carr, R.J. Shannon, B. Wang, M.A. Blitz, M.J. Pilling, et al, J. Phys. Chem. A **118** (2014) 6773.

- [35] D.J. Medeiros, M.A. Blitz, L. James, T.H. Speak, P.W. Seakins, *J. Phys. Chem. A* **122** (2018) 7239.
- [36] J. Troe, V.G. Ushakov, *Z. Phys. Chem. (Muenchen, Ger.)* **228** (2014) 1.
- [37] B. Ruscic, *Int. J. Quantum Chem.* **114** (2014) 1097.
- [38] B. Ruscic, D.H. Bross. Active Thermochemical Tables (ATcT) values based on ver. 1.122g of the Thermochemical Network [cited 2019] Available from: <https://atct.anl.gov/>
- [39] D.A. Good, J.S. Francisco, *Chem. Phys. Lett.* **266** (1997) 512.

## Supplementary Information

The MESMER fit to the data is given below, where the first 16 points are Leeds and the rest are Loucks and Laidler. This is followed by the best fit parameters together with the correlation matrix. PLOG parameterization of  $k_1(T,p)$  is also for the buffers gases: CH<sub>3</sub>OCH<sub>3</sub>, He and N<sub>2</sub>.

The xml MESMER input file for CH<sub>3</sub>OCH<sub>2</sub> is given at the end: **CH<sub>3</sub>OCH<sub>2</sub>\_xml**

### MESMER

Temperature	Concentration	Exp. Coeff	Cal. Coeff.
673	1.05E+17	1772	2011.63
673	1.05E+17	2520	2011.63
673	7.87E+17	7349	7590.4
673	7.87E+17	4777	7590.4
673	1.58E+18	13700	11400.9
673	4.01E+18	23275	18785.5
622	1.14E+17	951	559.68
622	1.14E+17	2747	559.68
622	8.50E+17	1948	1943.29
622	1.93E+18	3347	3015.4
622	1.70E+18	4151	2824.38
622	4.34E+18	5969	4438.47
573	1.23E+17	37.6921	123.697
573	9.24E+17	791	392.47
573	2.10E+18	767	584.095
573	1.85E+18	396	550.75
573	5.53E+16	155.681	113.469
573	9.13E+16	199.635	155.502
573	1.21E+17	179.571	184.114
573	2.49E+17	238.361	279.347
573	3.48E+17	264.994	335.367
573	5.42E+17	391.053	422.194
573	8.48E+17	641.558	524.977
573	9.47E+17	483.321	552.864
573	1.65E+18	665.635	708.163
573	4.03E+18	714.884	1002.96
543	6.16E+16	62.5794	42.469
543	9.63E+16	72.1824	55.3289
543	1.20E+17	80.2475	62.8739

543	2.22E+17	99.1817	87.8597
543	3.88E+17	110.263	116.609
543	6.77E+17	118.422	151.486
543	7.16E+17	146.363	155.281
543	1.12E+18	174.756	187.947
543	1.65E+18	208.656	219.693
543	2.57E+18	287.363	258.631
543	2.88E+18	330.698	268.925
543	3.05E+18	257.888	274.019
543	5.32E+18	408.725	326.788
521	6.80E+16	25.1082	18.793
521	1.12E+17	25.9905	24.8604
521	1.48E+17	28.9611	28.8608
521	1.75E+17	31.0324	31.5023
521	2.32E+17	35.7944	36.2729
521	3.42E+17	41.1922	43.7785
521	5.04E+17	42.7381	52.2771
521	5.97E+17	45.9003	56.251
521	7.46E+17	56.7303	61.8047
521	1.16E+18	65.2853	73.7225
521	1.82E+18	75.3035	86.7095
521	3.55E+18	96.564	107.42
521	6.54E+18	107.353	126.898
521	1.21E+19	132.683	145.853
498	6.02E+16	9.74255	6.3363
498	1.05E+17	10.4393	8.55305
498	1.83E+17	12.4644	11.3135
498	2.86E+17	14.8824	13.9261
498	4.99E+17	19.0841	17.7129
498	6.97E+17	21.2164	20.236
498	8.25E+17	21.2164	21.571
498	1.15E+18	23.587	24.3351
498	1.90E+18	27.2065	28.7098
498	3.14E+18	31.3092	33.2277
498	4.64E+18	37.3828	36.7308
498	8.10E+18	47.9372	41.5857
473	7.92E+16	3.39853	2.10681
473	9.88E+16	3.28315	2.35286
473	1.11E+17	3.77825	2.48616
473	2.04E+17	4.0578	3.30191
473	2.55E+17	4.84496	3.63763
473	5.55E+17	4.35803	4.95328
473	4.97E+17	5.20344	4.75389
473	7.77E+17	5.3863	5.58086
473	8.22E+17	5.3863	5.68671
473	9.70E+17	5.78483	6.00809
473	1.52E+18	6.65718	6.89523
473	2.65E+18	7.9486	8.01644
473	3.70E+18	8.53671	8.67736
473	5.45E+18	9.49053	9.42061
473	8.52E+18	10.9469	10.2193
473	1.19E+19	12.17	10.7674
473	1.26E+19	11.3316	10.8536

Chi^2 = 72.4903

### Best fit parameters:

CH3OCH2:deltaEDown:He	=	195.801	+/-	320.849
CH3OCH2:deltaEDown:CH3OCH3	=	871.511	+/-	611.272
CH3OCH2:deltaEDownTExponent:He	=	0.769149	+/-	2.0268
CH3OCH2:deltaEDownTExponent:CH3OCH3	=	-0.87181	+/-	1.00524
TS1:ZPE	=	128.512	+/-	0.581291

### CORRELATION MATRIX

Correlation		coefficients:		
CH3OCH2:deltaEDown:CH3OCH3	,	CH3OCH2:deltaEDown:He	=	0.134329
CH3OCH2:deltaEDownTExponent:He	,	CH3OCH2:deltaEDown:He	=	-0.99796
CH3OCH2:deltaEDownTExponent:He	,	CH3OCH2:deltaEDown:CH3OCH3	=	-0.10237
CH3OCH2:deltaEDownTExponent:CH3OCH3	,	CH3OCH2:deltaEDown:He	=	-0.11253
CH3OCH2:deltaEDownTExponent:CH3OCH3	,	CH3OCH2:deltaEDown:CH3OCH3	=	-0.98254
CH3OCH2:deltaEDownTExponent:CH3OCH3	,	CH3OCH2:deltaEDownTExponent:He	=	0.085754
TS1:ZPE	,	CH3OCH2:deltaEDown:He	=	0.177591
TS1:ZPE	,	CH3OCH2:deltaEDown:CH3OCH3	=	0.756393
TS1:ZPE	,	CH3OCH2:deltaEDownTExponent:He	=	-0.13534
TS1:ZPE	,	CH3OCH2:deltaEDownTExponent:CH3C	=	-0.63363

## PLOG

Bath	gas	is	CH3OCH3			
units(length	=	'cm',	quantity	=	'mole')	
pdep_arrhenius('CH3OCH2	=>	CH2O	+	CH3',		
		[( 0.001, 'atm'),	5.66189e+52,	-13.7666,	34561.6],	
		[( 0.01, 'atm'),	3.22796e+52,	-13.3182,	35451.7],	
		[( 0.1, 'atm'),	2.67855e+49,	-11.9866,	35643.6],	
		[( 1, 'atm'),	1.18294e+42,	-9.34681,	34514.1],	
		[( 10, 'atm'),	1.06617e+31,	-5.61002,	32056.1],	
		[( 100, 'atm'),	2.60276e+19,	-1.77664,	29124.8],	
		[( 1000, 'atm'),	1.00434e+11,	0.967752,	26874])	
Bath	gas	is	He			
units(length	=	'cm',	quantity	=	'mole')	
pdep_arrhenius('CH3OCH2	=>	CH2O	+	CH3',		
		[( 0.001, 'atm'),	3.56127e+36,	-8.51999,	30552],	
		[( 0.01, 'atm'),	3.47613e+36,	-8.17061,	31257.8],	
		[( 0.1, 'atm'),	7.28559e+34,	-7.30714,	31624.4],	
		[( 1, 'atm'),	2.50608e+30,	-5.59772,	31216.2],	
		[( 10, 'atm'),	6.97338e+22,	-2.97588,	29740.6],	
		[( 100, 'atm'),	2.75721e+14,	-0.172067,	27724.1],	
		[( 1000, 'atm'),	5.34256e+08,	1.70146,	26233.6])	
Bath	gas	is	N2			
units(length	=	'cm',	quantity	=	'mole')	
pdep_arrhenius('CH3OCH2	=>	CH2O	+	CH3',		
		[( 0.001, 'atm'),	5.13565e+39,	-9.48044,	31404.5],	
		[( 0.01, 'atm'),	3.54673e+39,	-9.07744,	32166.3],	
		[( 0.1, 'atm'),	1.70294e+37,	-8.0086,	32436.6],	
		[( 1, 'atm'),	3.20089e+31,	-5.90578,	31681.7],	
		[( 10, 'atm'),	5.11864e+22,	-2.90525,	29800.9],	
		[( 100, 'atm'),	7.46442e+13,	0.021111,	27602.8],	
		[( 1000, 'atm'),	2.51763e+08,	1.8091,	26150.2])	

## CH<sub>3</sub>OCH<sub>2</sub>\_xml

```

<moleculeList>
  <molecule xmlns="http://www.xml-cml.org/schema" id="CH3OCH2">
    <atomArray>
      <atom id="a1" elementType="C" x3="1.133135" y3="0.182321" z3="0.023603"/>
      <atom id="a2" elementType="H" x3="1.959364" y3="-0.507761" z3="-0.157056"/>
      <atom id="a3" elementType="H" x3="1.265317" y3="0.633497" z3="1.011781"/>
      <atom id="a4" elementType="H" x3="1.170775" y3="0.977813" z3="-0.727106"/>
      <atom id="a5" elementType="O" x3="-0.083811" y3="-0.575348" z3="-0.062825"/>
      <atom id="a6" elementType="C" spinMultiplicity="2" x3="-1.201238" y3="0.245941" z3="0.093580"/>
      <atom id="a7" elementType="H" x3="-2.137569" y3="-0.304197" z3="0.037680"/>
      <atom id="a8" elementType="H" x3="-1.178782" y3="1.233861" z3="-0.365804"/>
    </atomArray>
    <bondArray>
      <bond atomRefs2="a3 a1" order="1"/>
    </bondArray>
  </molecule>
</moleculeList>

```

```

<bond atomRefs2="a7 a6" order="1"/>
<bond atomRefs2="a2 a1" order="1"/>
<bond id="b1" atomRefs2="a5 a1" order="1"/>
<bond id="b2" atomRefs2="a5 a6" order="1"/>
<bond atomRefs2="a8 a6" order="1"/>
<bond atomRefs2="a1 a4" order="1"/>
</bondArray>
<propertyList>
<property title="program">
<scalar>Gaussian 09, Revision D.01</scalar>
</property>
<property title="basis">
<scalar>6-31+G(d,p) (6D, 7F)</scalar>
</property>
<property title="method">
<scalar>m062x</scalar>
</property>
<property title="File Format">
<scalar>g03</scalar>
</property>
<property title="Energy" dictRef="me:ZPE">
<scalar units="kJ/mol" >15.97</scalar>
</property>
<!-- <property dictRef="me:vibFreqs" > -->
<!-- <array units="cm-1" >199.43 281.27 502.82 892.66 1135.45 1259.58 1310.36 1428.28 1456.37 1724.45 1769.00
1803.41 1816.70 3523.42 3578.57 3691.43 3721.75 3760.59 </array> -->
<!-- </property> -->
<property title="Rotational Constants" dictRef="me:rotConsts">
<array units="cm-1" >1.468 0.354 0.305 </array>
</property>
<property dictRef="me:frequenciesScaleFactor">
<scalar>0.86</scalar>
</property>
<property title="Hessian" dictRef="me:hessian">
<matrix rows="24" matrixType="squareSymmetricLT" units="Hartree/Bohr2" >0.79827926 -0.05787253 0.84101881 -0.00540215
0.00658624 0.81400113 -0.27887837 0.18247961 0.04655398 0.30265882 0.18765979 -0.24288937 -0.04117453 -0.19090282
0.24008241 0.04743388 -0.04154478 -0.09366654 -0.04973823 0.04419587 0.07979925 -0.07940451 -0.00834751 -0.03544763
0.00845969 0.01039189 0.03183251 0.08105183 -0.01037969 -0.13863855 -0.13368942 -0.00620638 -0.00594536 -0.02625512
0.02293723 0.13740048 -0.03300529 -0.13055498 -0.38509290 -0.00381678 0.00391803 0.00033420 0.04055329 0.14587646
0.39499166 -0.07653780 0.00059747 0.00688843 0.00582782 0.02088519 -0.02569426 0.00272617 0.00417794 -0.00096626
0.07711457 -0.00071096 -0.26700514 0.18255902 -0.00495411 -0.01244062 0.02061202 0.00137059 0.01794079 -0.01766457
0.01333575 0.27899257 0.00444524 0.17983164 -0.25853536 0.00143781 -0.01158591 0.00975547 -0.00025944 0.03277297
-0.01853782 -0.00663748 -0.19664402 0.25730761 -0.30235601 -0.16711055 -0.02136813 -0.03196787 -0.02225366 -0.00267713
-0.01887827 -0.01351367 -0.00382374 -0.01586321 -0.01282733 0.00110781 0.72242512 -0.09020690 -0.20058248 -0.01689578
0.02331860 0.02358876 0.00366800 -0.02372859 -0.01072119 -0.00272916 -0.03407156 -0.01917162 -0.00317189 -0.00971125
0.44542320 -0.01316817 -0.01494517 -0.07370777 0.00539378 0.00500072 0.00267136 -0.03446643 -0.01915189 0.00721874
0.02549805 0.01234783 0.00969105 -0.01672942 0.03932161 0.07252495 -0.06320016 0.04075221 0.00951861 -0.00513742
-0.00455312 -0.00102683 0.00657518 0.00324845 0.00073103 0.00617951 0.00384006 0.00000621 -0.32832140 0.12237525
0.05339526 0.82788951 -0.02948419 0.01028582 0.00431495 -0.00465003 -0.00401871 -0.00069831 -0.00318124 -0.00003478
0.00140831 -0.00529937 0.00126574 -0.00112780 0.19859715 -0.24422995 -0.03598373 0.02710208 0.80163750 -0.00177177
0.00208810 -0.00508836 0.00010414 -0.00022927 0.00090913 -0.00243491 0.00044876 0.00127300 0.00172414 -0.00107107
0.00038506 0.04222984 -0.01901261 -0.02816136 -0.04317663 -0.13434643 0.15923118 -0.00338334 0.00448480 0.00098715
-0.00101204 -0.00098619 -0.00015711 0.00012579 0.00017249 0.00022592 0.00021002 0.00023424 -0.00012222 -0.02187857
-0.02044623 -0.00566446 -0.36090329 -0.16434143 -0.00810790 0.37927769 0.00367206 -0.00472804 -0.00082878 0.00125023
0.00153009 0.00013320 0.00029957 0.00004378 -0.00013979 0.00034629 0.00010527 -0.00001497 0.02608510 0.02177575
0.00175179 -0.17966863 -0.18633777 0.00551089 0.17468431 0.17190816 0.00241240 -0.00079660 0.00194813 0.00015479
0.00011700 0.00019690 0.00005658 -0.00006820 -0.00004636 -0.00032897 -0.00034617 0.00003816 0.00221232 0.00731404
0.00167811 -0.03817613 -0.01795105 -0.02598330 0.01765448 0.00218432 0.01673540 0.00548093 0.00501650 -0.00173026
0.00004938 -0.00024107 0.00002717 -0.00065587 -0.00043637 0.00010182 0.00034293 -0.00028824 0.00002208 -0.00315979
0.03247069 -0.01425861 -0.08308193 -0.01874297 0.01143309 0.00756376 -0.02666893 0.01601452 0.07346059 -0.00267757
0.00253895 -0.00087171 -0.00033510 0.00009281 -0.00011088 0.00025807 -0.00004517 -0.00011430 0.00002829 0.00031302
-0.00006002 0.00073422 -0.01608247 0.01165884 -0.01309631 -0.37856785 0.14661163 0.00619801 -0.00429724 0.00954666
0.00889040 0.39604796 -0.00094415 -0.00066445 0.00014167 -0.00008948 -0.00024192 0.00000023 0.00016602 0.00006644
-0.00014053 -0.00048366 0.00020697 -0.00010417 -0.00095155 -0.00849420 0.00808491 0.01872847 0.18438406 -0.10256536
-0.00481585 -0.00859667 0.00543296 -0.01160981 -0.16666023 0.08915028 </matrix>
</property>

<property dictRef="me:sigma">
<scalar>4.98</scalar>
</property>
<property dictRef="me:epsilon">
```

```

<scalar>329.669</scalar>
</property>

<property title="Symmetry Number" dictRef="me:symmetryNumber">
<scalar>1 </scalar>
</property>
<property dictRef="me:spinMultiplicity">
<scalar>2</scalar>

    <property dictRef="me:MW">
    <scalar units="amu">45</scalar>
    </property>

</property>
</propertyList>
<me:DOSCMETHOD>Classical rotors</me:DOSCMETHOD>
<me:ExtraDOSCMETHOD xsi:type="HinderedRotorQM1D">
<me:bondRef>b1</me:bondRef>
<me:HinderedRotorPotential format="numerical" units="kJ/mol" expansionSize="7" useSineTerms="yes" scale="1">
<me:PotentialPoint angle=" 0 " potential=" 0 " />
<me:PotentialPoint angle=" 30 " potential=" 3.536157301 " />
<me:PotentialPoint angle=" 60 " potential=" 6.415658673 " />
<me:PotentialPoint angle=" 90 " potential=" 2.985975899 " />
<me:PotentialPoint angle=" 120 " potential=" -0.018026683 " />
<me:PotentialPoint angle=" 150 " potential=" 3.293679248 " />
<me:PotentialPoint angle=" 180 " potential=" 6.422936558 " />
<me:PotentialPoint angle=" 210 " potential=" 2.917500234 " />
<me:PotentialPoint angle=" 240 " potential=" -0.008288703 " />
<me:PotentialPoint angle=" 270 " potential=" 3.433744422 " />
<me:PotentialPoint angle=" 300 " potential=" 6.413828699 " />
<me:PotentialPoint angle=" 330 " potential=" 2.809579056 " />
<me:PotentialPoint angle=" 360 " potential=" 1.989063047 " />
</me:HinderedRotorPotential>
<me:periodicity>3</me:periodicity>
</me:ExtraDOSCMETHOD>
<me:ExtraDOSCMETHOD xsi:type="HinderedRotorQM1D">
<me:bondRef>b2</me:bondRef>
<me:HinderedRotorPotential format="numerical" units="kJ/mol" expansionSize="7" useSineTerms="yes" scale="1">
<me:PotentialPoint angle=" 0 " potential=" 1.978445525 " />
<me:PotentialPoint angle=" 30 " potential=" 0 " />
<me:PotentialPoint angle=" 60 " potential=" 6.721521546 " />
<me:PotentialPoint angle=" 90 " potential=" 20.83341076 " />
<me:PotentialPoint angle=" 120 " potential=" 13.52849261 " />
<me:PotentialPoint angle=" 150 " potential=" 4.067975955 " />
<me:PotentialPoint angle=" 180 " potential=" 0.008196811 " />
<me:PotentialPoint angle=" 210 " potential=" 4.067975955 " />
<me:PotentialPoint angle=" 240 " potential=" 13.52851099 " />
<me:PotentialPoint angle=" 270 " potential=" 22.24308635 " />
<me:PotentialPoint angle=" 300 " potential=" 6.721539925 " />
<me:PotentialPoint angle=" 330 " potential=" 2.62557E-06 " />
<me:PotentialPoint angle=" 360 " potential=" 1.978445525 " />
</me:HinderedRotorPotential>
<me:periodicity>2</me:periodicity>
</me:ExtraDOSCMETHOD>
<me:energyTransferModel xsi:type="me:ExponentialDown">

    <!-- <me:deltaEDown bathGas="N2" units="cm-1" lower="50" upper="800" stepsize="10">523</me:deltaEDown> --
>
    <!-- <me:deltaEDownTExponent bathGas="N2" lower="-1.0" upper="1.5"
stepsize="0.01">0.25</me:deltaEDownTExponent> -->

<me:deltaEDown bathGas="N2" units="cm-1" >523</me:deltaEDown>
<me:deltaEDownTExponent bathGas="N2" >0.25</me:deltaEDownTExponent>
<me:deltaEDown bathGas="He" units="cm-1" lower="50" upper="400" stepsize="10">120</me:deltaEDown>
    <me:deltaEDownTExponent bathGas="He" lower="0.75" upper="1.5"
stepsize="0.01">1.00</me:deltaEDownTExponent>

        <me:deltaEDown bathGas="CH3OCH3" units="cm-1" lower="300" upper="4000"
stepsize="10">600</me:deltaEDown>
            <me:deltaEDownTExponent bathGas="CH3OCH3" referenceTemperature="521" lower="-1.0" upper="4.0" stepsize="0.01">-.58</me:deltaEDownTExponent>

```

```

</me:energyTransferModel>
</molecule>

<molecule xmlns="http://www.xml-cml.org/schema" id="TS1">
<atomArray>
<atom id="a1" elementType="C" spinMultiplicity="2" x3="-1.182055" y3="-0.899551" z3="0.000000"/>
<atom id="a2" elementType="H" x3="-2.126915" y3="-0.373171" z3="0.000000"/>
<atom id="a3" elementType="H" x3="-0.890176" y3="-1.381789" z3="0.924593"/>
<atom id="a4" elementType="H" x3="-0.890176" y3="-1.381789" z3="-0.924593"/>
<atom id="a5" elementType="O" x3="0.000000" y3="0.641527" z3="0.000000"/>
<atom id="a6" elementType="C" x3="1.237194" y3="0.454609" z3="0.000000"/>
<atom id="a7" elementType="H" x3="1.788219" y3="0.337093" z3="0.941064"/>
<atom id="a8" elementType="H" x3="1.788219" y3="0.337093" z3="-0.941064"/>
</atomArray>
<bondArray>
<bond atomRefs2="a8 a6" order="1"/>
<bond atomRefs2="a4 a1" order="1"/>
<bond atomRefs2="a1 a2" order="1"/>
<bond atomRefs2="a1 a3" order="1"/>
<bond id="b2" atomRefs2="a5 a6" order="2"/>
<bond atomRefs2="a6 a7" order="1"/>
<bond id="b1" atomRefs2="a1 a5" order="1"/>
</bondArray>
<propertyList>
<property title="Energy" dictRef="me:ZPE">
<scalar units="kJ/mol" >128.512</scalar>
<!-- <scalar units="kJ/mol" lower="80" upper="150" stepsize="0.2">124.257</scalar> -->
</property>
<!-- <property dictRef="me:vibFreqs"> -->
<!-- <array units="cm-1">91.28 219.31 282.03 653.61 672.59 956.62 983.61 1225.73 1373.83 1438.19 1443.80
      1571.36 3035.92 3132.81 3139.38 3306.96 3320.39 </array> -->
<!-- </property> -->
<property dictRef="me:frequenciesScaleFactor">
<scalar>0.86</scalar>
</property>
<property title="Hessian" dictRef="me:hessian">
<matrix rows="24" matrixType="squareSymmetricLT" units="Hartree/Bohr2">0.04187327 -0.22856471 0.54873352
          0.00000000 0.00000000 0.62248689 -0.10633956 0.15258347 0.00000000 0.11098361 0.14406444 -
0.27904298
          0.00000000 -0.15357996 0.28920075 0.00000000 0.00000000 -0.05394579 0.00000000 0.00000000
0.04638704
          -0.02537317 0.01202436 0.00209982 0.00414276 0.00771498 -0.01426636 0.02564458 0.01717287 -
0.13238216
          0.13769825 -0.00205025 -0.00713713 0.02087588 -0.01206360 0.13045441 -0.00734009 0.13422194 -
0.27811654
          0.00134057 -0.00311257 0.00386913 0.00533858 -0.14471796 0.28593480 -0.02537317 0.01202436 -
0.00209982
          0.00414276 0.00771498 0.01426636 0.00295815 0.00029531 0.00035293 0.02564458 0.01717287 -
0.13238216
          -0.13769825 -0.00205025 -0.00713713 -0.02087588 0.00029531 0.01109441 0.01504803 -0.01206360
0.13045441
          0.00734009 -0.13422194 -0.27811654 -0.00134057 0.00311257 0.00386913 -0.00035293 -0.01504803 -
0.01386194
          -0.00533858 0.14471796 0.28593480 0.24300314 0.07887203 0.00000000 -0.00874822 -0.00313341
0.00000000
          -0.00953898 -0.00370953 -0.00084307 -0.00953898 -0.00370953 0.00084307 0.03328285 -0.05453287 -
0.04944329
          0.00000000 0.00762654 0.00376089 0.00000000 -0.00719787 -0.00193518 -0.00116772 -0.00719787 -
0.00193518
          0.00116772 -0.22698969 0.31823568 0.00000000 0.00000000 -0.01257802 0.00000000 0.00000000 -
0.00000489
          0.00634176 0.00128923 0.00236996 -0.00634176 -0.00128923 0.00236996 0.00000000 0.00000000
0.07163447
          -0.13556599 -0.03027554 0.00000000 -0.00426889 -0.00259854 0.00000000 0.00268694 0.00070361
0.00103045
          0.00268694 0.00070361 -0.00103045 -0.20311858 0.23695616 0.00000000 0.48791588 0.10528816
0.04471924
          0.00000000 -0.00281856 0.00024532 0.00000000 -0.00118392 -0.00020305 -0.00040897 -0.00118392 -
0.00020305

```

```

0.00040897 0.11490841 -0.25215447 0.00000000 -0.27733168 0.33925142 0.00000000 0.00000000 -
0.00014693 0.00000000 0.00000000 -0.00031628 0.00144747 -0.00013442 0.00002505 -0.00144747 0.00013442
0.00002505 0.00000000 0.00000000 -0.09073850 0.00000000 0.00000000 0.61970144 0.00388773 0.00166801 -
0.00125162 0.00004377 -0.00009125 0.00004112 -0.00007251 -0.00024785 0.00018716 -0.00044777 -0.00010057
0.00006653 -0.02267062 0.02566780 -0.02592572 -0.07516815 0.03116075 -0.07110018 0.08375195 -0.00030038 -
0.00010109 -0.00051746 0.00014451 0.00005514 0.00000364 0.00037709 0.00008648 0.00004514 0.00003365
0.00002221 -0.00009209 0.02188085 -0.00826423 0.02154335 0.03592119 -0.06582771 0.06816844 -0.05936305
0.06376559 0.00398565 0.00102016 0.00020847 0.00009279 -0.00001367 0.00007082 -0.00050858 0.00007536 -
0.00013205 0.00009976 0.00003830 -0.00008840 -0.01561559 0.00877309 0.01347351 -0.06814220 0.06235674 -
0.26427491 0.08903544 -0.08070051 0.26674313 0.00388773 0.00166801 0.00125162 0.00004377 -0.00009125 -
0.00004112 -0.00044777 -0.00010057 -0.00006653 -0.00007251 -0.00024785 -0.00018716 -0.02267062 0.02566780
0.02592571 -0.07516815 0.03116075 0.07110018 0.01067561 0.00130615 -0.00894727 0.08375195 -0.00030038 -
0.00010109 0.00051746 0.00014450 0.00005514 -0.00000364 0.00003365 0.00002221 0.00009209 0.00037709
0.00008648 -0.00004514 0.02188085 -0.00826423 -0.02154335 0.03592119 -0.06582771 -0.06816844 0.00130615
0.01026359 0.00845052 -0.05936305 0.06376559 -0.00398565 -0.00102016 0.00020847 -0.00009279 0.00001367
0.00007082 -0.00009976 -0.00003830 -0.00008840 0.00050858 -0.00007536 -0.00013205 0.01561559 -0.00877309
0.01347351 0.06814220 -0.06235674 -0.26427491 0.00894727 -0.00845052 -0.01600057 -0.08903544 0.08070051
0.26674313 </matrix>
</property>
<property title="ImaginaryFrequency" dictRef="me:imFreqs">
<scalar units="cm-1">767.74 </scalar>
</property>
<property title="Rotational Constants" dictRef="me:rotConsts">
<array units="cm-1">1.429 0.256 0.239 </array>
</property>

<property dictRef="me:spinMultiplicity">
<scalar>2</scalar>
</property>
<property title="Symmetry Number" dictRef="me:symmetryNumber">
<scalar>1 </scalar>
</property>

<property dictRef="me:MW">
<scalar units="amu">45</scalar>
</property>

</propertyList>
<me:DOSCMETHOD>Classical rotors</me:DOSCMETHOD>
<me:ExtraDOSCMETHOD xs:type="HinderedRotorQM1D">
<me:bondRef>b1</me:bondRef>
<me:HinderedRotorPotential format="numerical" units="kJ/mol" expansionSize="7" useSineTerms="yes" scale="1">
<me:PotentialPoint angle=" 0 " potential=" 0 " />
<me:PotentialPoint angle=" 30 " potential=" 0.918772721 " />
<me:PotentialPoint angle=" 60 " potential=" 1.598958381 " />
<me:PotentialPoint angle=" 90 " potential=" 0.678276921 " />
<me:PotentialPoint angle=" 120 " potential=" 0.005445287 " />
<me:PotentialPoint angle=" 150 " potential=" 0.925375853 " />
<me:PotentialPoint angle=" 180 " potential=" 1.598055209 " />
<me:PotentialPoint angle=" 210 " potential=" 0.702063951 " />
<me:PotentialPoint angle=" 240 " potential=" -0.003273999 " />
<me:PotentialPoint angle=" 270 " potential=" 0.898149419 " />
<me:PotentialPoint angle=" 300 " potential=" 1.59922093 " />

```

```

<me:PotentialPoint      angle=" 330      " potential="      0.693242271      " />
<me:PotentialPoint      angle=" 360      " potential="      0      " />
</me:HinderedRotorPotential>
<me:periodicity>3</me:periodicity>
</me:ExtraDOSCMETHOD>
<me:ExtraDOSCMETHOD xsi:type="HinderedRotorQM1D">
<me:bondRef>b2</me:bondRef>
<me:HinderedRotorPotential format="numerical" units="kJ/mol" expansionSize="7" useSineTerms="yes" scale="1">
<me:PotentialPoint      angle=" 0      " potential="      4.785355356      " />
<me:PotentialPoint      angle=" 30      " potential="      0      " />
<me:PotentialPoint      angle=" 60      " potential="      16.25764709      " />
<me:PotentialPoint      angle=" 90      " potential="      50.39070953      " />
<me:PotentialPoint      angle=" 120      " potential="      32.72197479      " />
<me:PotentialPoint      angle=" 150      " potential="      9.839396777      " />
<me:PotentialPoint      angle=" 180      " potential="      0.019825996      " />
<me:PotentialPoint      angle=" 210      " potential="      9.839396777      " />
<me:PotentialPoint      angle=" 240      " potential="      32.72201924      " />
<me:PotentialPoint      angle=" 270      " potential="      53.80035539      " />
<me:PotentialPoint      angle=" 300      " potential="      16.25769154      " />
<me:PotentialPoint      angle=" 330      " potential="      6.35059E-06      " />
<me:PotentialPoint      angle=" 360      " potential="      4.785355356      " />
</me:HinderedRotorPotential>
<me:periodicity>2</me:periodicity>
</me:ExtraDOSCMETHOD>
</molecule>

<molecule id="CH3">
<atomArray>
<atom id="a1" elementType="C" spinMultiplicity="2" x2="0.000000" y2="0.000000"/>
<atom id="a2" elementType="H" x2="0.000000" y2="1.078800"/>
<atom id="a3" elementType="H" x2="0.934300" y2="-0.539400"/>
<atom id="a4" elementType="H" x2="-0.934300" y2="-0.539400"/>
</atomArray>
<bondArray>
<bond atomRefs2="a1 a2" order="1"/>
<bond atomRefs2="a1 a3" order="1"/>
<bond atomRefs2="a1 a4" order="1"/>
</bondArray>
<propertyList>
<property dictRef="me:ZPE">
<scalar units="kJ/mol">149.872</scalar>
</property>
<property dictRef="me:rotConsts">
<array units="cm-1">9.57789 9.57789 4.74202</array>
</property>
<property dictRef="me:symmetryNumber">
<scalar>6</scalar>
</property>
<property dictRef="me:vibFreqs">
<array units="cm-1">3004 606 3161 3161 1396 1396</array>
</property>
<property dictRef="me:MW">
<scalar units="amu">15</scalar>
</property>
<property dictRef="me:epsilon">
<scalar>140</scalar>
</property>
<property dictRef="me:sigma">
<scalar>3.8</scalar>
</property>
<property dictRef="me:spinMultiplicity">
<scalar>2</scalar>
</property>
</propertyList>
<me:DOSCMETHOD name="QMRotors" />
<!--me:DOSCMETHOD name="ClassicalRotors"-->
<me:energyTransferModel xsi:type="me:ExponentialDown">
<me:deltaEDown bathGas="N2" units="cm-1" lower="50" upper="800" stepsize="10">370</me:deltaEDown>
<me:deltaEDownTExponent bathGas="N2" lower="-1.0" upper="1.5"
stepsize="0.01">0.57</me:deltaEDownTExponent>

```

```

<!-- <me:deltaEDown bathGas="N2" units="cm-1" >250</me:deltaEDown> -->
<!-- <me:deltaEDownTExponent bathGas="N2" >0.25</me:deltaEDownTExponent> -->
<me:deltaEDown bathGas="He" units="cm-1" lower="50" upper="400" stepsize="10">192.511</me:deltaEDown>
    <me:deltaEDownTExponent bathGas="He" lower="0.75" upper="1.5"
stepsize="0.01">0.75</me:deltaEDownTExponent>

        <me:deltaEDown bathGas="CH3OCH3" units="cm-1" lower="300" upper="4000"
stepsize="10">848</me:deltaEDown>
            <me:deltaEDownTExponent bathGas="CH3OCH3" referenceTemperature="521" lower="-1.0"
upper="4.0" stepsize="0.01">-.58</me:deltaEDownTExponent>
        </me:energyTransferModel>
    </molecule>

    <molecule xmlns="http://www.xml-cml.org/schema" id="CH2O">
<atomArray>
<atom id="a1" elementType="O" x3="0.000000" y3="-0.674346" z3="0.000000"/>
<atom id="a2" elementType="C" x3="0.000000" y3="0.529185" z3="0.000000"/>
<atom id="a3" elementType="H" x3="-0.940850" y3="1.109829" z3="0.000000"/>
<atom id="a4" elementType="H" x3="0.940850" y3="1.109829" z3="0.000000"/>
</atomArray>
<bondArray>
<bond atomRefs2="a1 a2" order="2"/>
<bond atomRefs2="a2 a3" order="1"/>
<bond atomRefs2="a2 a4" order="1"/>
</bondArray>
<propertyList>
<property title="Energy" dictRef="me:ZPE">
    <scalar units="kJ/mol">-105.379</scalar>
</property>
<property dictRef="me:vibFreqs">
    <array units="cm-1">2782 1746 1500 1167 2843 1249</array>
</property>
<property title="Rotational Constants" dictRef="me:rotConsts">
    <array units="cm-1">9.4053 1.29530 1.13420</array>
</property>
<property title="Symmetry Number" dictRef="me:symmetryNumber">
    <scalar>2 </scalar>
</property>
    <property dictRef="me:spinMultiplicity">
        <scalar>1</scalar>
    </property>
    <property dictRef="me:MW">
        <scalar units="amu">30</scalar>
    </property>
    <property dictRef="me:epsilon">
        <scalar>140</scalar>
    </property>
    <property dictRef="me:sigma">
        <scalar>3.8</scalar>
    </property>
</propertyList>
<me:DOSCMETHOD name="QMROtors" />
<me:energyTransferModel xsi:type="me:ExponentialDown">
    <me:deltaEDown bathGas="N2" units="cm-1" lower="50" upper="800" stepsize="10">370</me:deltaEDown>
    <me:deltaEDownTExponent bathGas="N2" lower="-1.0" upper="1.5"
stepsize="0.01">0.57</me:deltaEDownTExponent>

        <!-- <me:deltaEDown bathGas="N2" units="cm-1" >250</me:deltaEDown> -->
        <!-- <me:deltaEDownTExponent bathGas="N2" >0.25</me:deltaEDownTExponent> -->
        <me:deltaEDown bathGas="He" units="cm-1" lower="50" upper="400" stepsize="10">192.511</me:deltaEDown>
            <me:deltaEDownTExponent bathGas="He" lower="0.75" upper="1.5"
stepsize="0.01">0.75</me:deltaEDownTExponent>

                <me:deltaEDown bathGas="CH3OCH3" units="cm-1" lower="300" upper="4000"
stepsize="10">848</me:deltaEDown>
                    <me:deltaEDownTExponent bathGas="CH3OCH3" referenceTemperature="521" lower="-1.0" upper="4.0" stepsize="0.01">-.58</me:deltaEDownTExponent>
                </me:energyTransferModel>
            </molecule>

```

```

<molecule id="He">
<atom elementType="He"/>
<propertyList>
<property dictRef="me:epsilon">
<scalar>10.22</scalar>
</property>
<property dictRef="me:sigma">
<scalar>2.511</scalar>
</property>
<property dictRef="me:MW">
<scalar>4.04</scalar>
</property>
</propertyList>
</molecule>

<molecule id="N2">
<atom elementType="N" />
<propertyList>
<property dictRef="me:epsilon">
<scalar>48.0</scalar>
</property>
<property dictRef="me:sigma">
<scalar>3.90</scalar>
</property>
<property dictRef="me:MW">
<scalar units="amu">28.0</scalar>
</property>
</propertyList>
</molecule>

<molecule xmlns="http://www.xml-cml.org/schema" id="CH3OCH3">
<atomArray>
<atom id="a1" elementType="O" x3="0.000000" y3="0.000000" z3="0.601650"/>
<atom id="a2" elementType="C" x3="0.000000" y3="1.168190" z3="-0.200301"/>
<atom id="a3" elementType="C" x3="0.000000" y3="-1.168190" z3="-0.200301"/>
<atom id="a4" elementType="H" x3="0.000000" y3="2.020879" z3="0.477032"/>
<atom id="a5" elementType="H" x3="0.000000" y3="-2.020879" z3="0.477032"/>
<atom id="a6" elementType="H" x3="0.890226" y3="1.216521" z3="-0.840911"/>
<atom id="a7" elementType="H" x3="-0.890226" y3="1.216521" z3="-0.840911"/>
<atom id="a8" elementType="H" x3="-0.890226" y3="-1.216521" z3="-0.840911"/>
<atom id="a9" elementType="H" x3="0.890226" y3="-1.216521" z3="-0.840911"/>
</atomArray>
<bondArray>
<bond atomRefs2="a6 a2" order="1"/>
<bond atomRefs2="a7 a2" order="1"/>
<bond atomRefs2="a8 a3" order="1"/>
<bond atomRefs2="a9 a3" order="1"/>
<bond atomRefs2="a2 a4" order="1"/>
<bond atomRefs2="a2 a1" order="1"/>
<bond atomRefs2="a3 a5" order="1"/>
<bond atomRefs2="a3 a1" order="1"/>
</bondArray>
<propertyList>

<property dictRef="me:ZPE">
<scalar units="kJ/mol">-166.38</scalar>
</property>

<property title="Vibrational Frequencies" dictRef="me:vibFreqs">
<array units="cm-1">210.80 260.34 424.16 964.14 1140.18 1181.64 1219.84 1224.19 1292.45 1495.92 1532.37
1533.15 1543.58 1553.14 1569.46 3031.80 3042.98 3093.78 3097.09 3192.86 3194.79 </array>
</property>

<property title="Rotational Constants" dictRef="me:rotConsts">
<array units="cm-1">1.283 0.336 0.296 </array>
</property>

<property dictRef="me:sigma">
<scalar>4.98</scalar>
</property>

```

```

<property dictRef="me:epsilon">
  <scalar>329.669</scalar>
</property>

<property title="Symmetry Number" dictRef="me:symmetryNumber">
  <scalar>2</scalar>

<property dictRef="me:MW">
  <scalar units="amu">46.0</scalar>
</property>

</property>
</propertyList>
</molecule>

</moleculeList>

<reactionList>
  <reaction id="R1">
    <reactant>
      <molecule ref="CH3OCH2" me:type="modelled"/>
    </reactant>
    <product>
      <molecule ref="CH2O" me:type="sink"/>
    </product>
    <product>
      <molecule ref="CH3" me:type="sink"/>
    </product>
    <me:transitionState>
      <molecule ref="TS1" me:type="transitionState"/>
    </me:transitionState>
    <!-- <me:tunneling name="Eckart"/> -->
    <me:MCRCMethod>SimpleRRKM</me:MCRCMethod>
  </reaction>
</reactionList>

<me:conditions>
  <me:bathGas>N2</me:bathGas>
  <me:PTs>

    <!-- 300 s-1 propagated into the all errors and minus 200 s-1 -->
    <me:PTpair me:units="PPCC" me:P=" 1.05147E17" me:T=" 673 " ><me:bathGas>He</me:bathGas> <me:experimentalRate ref1="CH3OCH2" ref2="CH3OCH2" error="500"> 1772
    </me:experimentalRate> </me:PTpair>
    <me:PTpair me:units="PPCC" me:P=" 1.05147E17 " me:T=" 673 " ><me:bathGas>He</me:bathGas> <me:experimentalRate ref1="CH3OCH2" ref2="CH3OCH2" error="500"> 2520
    </me:experimentalRate> </me:PTpair>
    <me:PTpair me:units="PPCC" me:P=" 7.86525E17 " me:T=" 673 " ><me:bathGas>He</me:bathGas> <me:experimentalRate ref1="CH3OCH2" ref2="CH3OCH2" error="500"> 7349
    </me:experimentalRate> </me:PTpair>
    <me:PTpair me:units="PPCC" me:P=" 7.86525E17 " me:T=" 673 " ><me:bathGas>He</me:bathGas> <me:experimentalRate ref1="CH3OCH2" ref2="CH3OCH2" error="500"> 4777
    </me:experimentalRate> </me:PTpair>
    <me:PTpair me:units="PPCC" me:P=" 1.57549E18 " me:T=" 673 " ><me:bathGas>He</me:bathGas> <me:experimentalRate ref1="CH3OCH2" ref2="CH3OCH2" error="500"> 13700
    </me:experimentalRate> </me:PTpair>
    <me:PTpair me:units="PPCC" me:P=" 4.0141E18 " me:T=" 673 " ><me:bathGas>He</me:bathGas> <me:experimentalRate ref1="CH3OCH2" ref2="CH3OCH2" error="500"> 23275
    </me:experimentalRate> </me:PTpair>
    <me:PTpair me:units="PPCC" me:P=" 1.13586E17 " me:T=" 622 " ><me:bathGas>He</me:bathGas> <me:experimentalRate ref1="CH3OCH2" ref2="CH3OCH2" error="500"> 951
    </me:experimentalRate> </me:PTpair>
    <me:PTpair me:units="PPCC" me:P=" 1.13586E17 " me:T=" 622 " ><me:bathGas>He</me:bathGas> <me:experimentalRate ref1="CH3OCH2" ref2="CH3OCH2" error="500"> 2747
    </me:experimentalRate> </me:PTpair>
    <me:PTpair me:units="PPCC" me:P=" 8.49649E17 " me:T=" 622 " ><me:bathGas>He</me:bathGas> <me:experimentalRate ref1="CH3OCH2" ref2="CH3OCH2" error="500"> 1948
    </me:experimentalRate> </me:PTpair>
    <me:PTpair me:units="PPCC" me:P=" 1.93437E18 " me:T=" 622 " ><me:bathGas>He</me:bathGas> <me:experimentalRate ref1="CH3OCH2" ref2="CH3OCH2" error="500"> 3347
    </me:experimentalRate> </me:PTpair>
    <me:PTpair me:units="PPCC" me:P=" 1.70193E18 " me:T=" 622 " ><me:bathGas>He</me:bathGas> <me:experimentalRate ref1="CH3OCH2" ref2="CH3OCH2" error="500"> 4151
    </me:experimentalRate> </me:PTpair>
    <me:PTpair me:units="PPCC" me:P=" 4.33626E18 " me:T=" 622 " ><me:bathGas>He</me:bathGas> <me:experimentalRate ref1="CH3OCH2" ref2="CH3OCH2" error="500"> 5969
    </me:experimentalRate> </me:PTpair>
    <me:PTpair me:units="PPCC" me:P=" 37.69215 " me:T=" 573 " ><me:bathGas>He</me:bathGas> <me:experimentalRate ref1="CH3OCH2" ref2="CH3OCH2" error="500"> 304
    </me:experimentalRate> </me:PTpair>

```





```

<me:PTpair me:units="PPCC" me:P=" 9.69764E17 " me:T=" 473 ">
  <me:experimentalRate ref1="CH3OCH2" ref2="CH3OCH2" error=" 1.15697 ">
    5.78483 </me:experimentalRate> </me:PTpair>
<me:PTpair me:units="PPCC" me:P=" 1.51588E18 " me:T=" 473 ">
  <me:experimentalRate ref1="CH3OCH2" ref2="CH3OCH2" error=" 1.33144 ">
    6.65718 </me:experimentalRate> </me:PTpair>
<me:PTpair me:units="PPCC" me:P=" 2.64647E18 " me:T=" 473 ">
  <me:experimentalRate ref1="CH3OCH2" ref2="CH3OCH2" error=" 1.58972 ">
    </me:experimentalRate> </me:PTpair>
<me:PTpair me:units="PPCC" me:P=" 3.69544E18 " me:T=" 473 ">
  <me:experimentalRate ref1="CH3OCH2" ref2="CH3OCH2" error=" 1.70734 ">
    8.53671 </me:experimentalRate> </me:PTpair>
<me:PTpair me:units="PPCC" me:P=" 5.45339E18 " me:T=" 473 ">
  <me:experimentalRate ref1="CH3OCH2" ref2="CH3OCH2" error=" 1.89811 ">
    9.49053 </me:experimentalRate> </me:PTpair>
<me:PTpair me:units="PPCC" me:P=" 8.52445E18 " me:T=" 473 ">
  <me:experimentalRate ref1="CH3OCH2" ref2="CH3OCH2" error=" 2.18938 ">
    10.94689 </me:experimentalRate> </me:PTpair>
<me:PTpair me:units="PPCC" me:P=" 1.19033E19 " me:T=" 473 ">
  <me:experimentalRate ref1="CH3OCH2" ref2="CH3OCH2" error=" 2.434 ">
    </me:experimentalRate> </me:PTpair>
<me:PTpair me:units="PPCC" me:P=" 1.25796E19 " me:T=" 473 ">
  <me:experimentalRate ref1="CH3OCH2" ref2="CH3OCH2" error=" 2.26632 ">
    11.33158 </me:experimentalRate> </me:PTpair>

</me:PTs>
</me:conditions>

<me:modelParameters>
  <me:grainSize units="cm-1">80</me:grainSize>
  <me:energyAboveTheTopHill>25.0</me:energyAboveTheTopHill>
</me:modelParameters>

<me:control>
  <me:calcMethod xsi:type="me:marquardt">
    <me:MarquardtIterations>30</me:MarquardtIterations>
    <me:MarquardtTolerance>1e-6</me:MarquardtTolerance>
    <me:MarquardtDerivDelta>0.025</me:MarquardtDerivDelta>
  </me:calcMethod>

  <me:printSpeciesProfile/>
  <me:eigenvalues>1</me:eigenvalues>
</me:control>

  <me:control>
    <me:calcMethod units="kJ/mol" xsi:type="me:ThermodynamicTable">
      <me:Tmin>0</me:Tmin>
      <me:Tmid>500</me:Tmid>
      <me:Tmax>1000</me:Tmax>
      <me:Tstep>10</me:Tstep>
    </me:calcMethod>
  </me:control>

<me:control>
  <me:calcMethod xsi:type="me:analyticalRepresentation">
    <me:format representation ="Plog" rateUnits="cm3mole-1s-1">cantera</me:format>
    <me:precision>dd</me:precision>
    <me:plogNumTemp>8</me:plogNumTemp>

    <me:plogMaxTemp>1000</me:plogMaxTemp>
    <me:plogMinTemp>300</me:plogMinTemp>
    <me:plogConcs units="atm">
      <me:plogConc>0.001</me:plogConc>
      <me:plogConc>0.01</me:plogConc>
      <me:plogConc>0.1</me:plogConc>
      <me:plogConc>1</me:plogConc>
      <me:plogConc>10</me:plogConc>
        <me:plogConc>100</me:plogConc>
        <me:plogConc>1000</me:plogConc>
    </me:plogConcs>
    <me:doForAllBathGases/>
  </me:calcMethod>
  <me:eigenvalues>1</me:eigenvalues>
</me:control>
</me:mesmer>

```